Special Section: Vadose Zone Modeling
Vadose Zone Journal

Colloid Transport and Retention in Unsaturated Porous Media: A Review of Interface-, Collector-, and Pore-Scale Processes and Models

Scott A. Bradford* and Saeed Torkzaban

Our ability to accurately simulate the transport and retention of colloids in the vadose zone is currently limited by our lack of basic understanding of colloid retention processes that occur at the pore scale. This review discusses our current knowledge of physical and chemical mechanisms, factors, and models of colloid transport and retention at the interface, collector, and pore scales. The interface scale is well suited for studying the interaction energy and hydrodynamic forces and torques that act on colloids near interfaces. Solid surface roughness is reported to have a significant influence on both adhesive and applied hydrodynamic forces and torques, whereas non-Derjaguin–Landau–Verwey–Overbeek (DLVO) forces such as hydrophobic and capillary forces are likely to play a significant role in colloid interactions with the air–water interface. The flow field can be solved and mass transfer processes can be quantified at the collector scale. Here the potential for colloid attachment in the presence of hydrodynamic forces is determined from a balance of applied and adhesive torques. The fraction of the collector surface that contributes to attachment has been demonstrated to depend on both physical and chemical conditions. Processes of colloid mass transfer and retention can also be calculated at the pore scale. Differences in collector- and pore-scale studies occur as a result of the presence of small pore spaces that are associated with multiple interfaces and zones of relative flow stagnation. Here a variety of straining processes may occur in saturated and unsaturated systems, as well as colloid size exclusion. Our current knowledge of straining processes is still incomplete, but recent research indicates a strong coupling of hydrodynamics, solution chemistry, and colloid concentration on these processes, as well as a dependency on the size of the colloid, the solid grain, and the water content.

Abbreviations: AWI, air–water interface; DLVO, Derjaguin–Landau–Verwey–Overbeek; SWI, solid–water interface.

Colloids are particles with effective diameters of around 10 nm to 10 μm. The lower limit of this size range corresponds to particles that are just larger than dissolved macromolecules and the upper limit to suspended particles that resist rapid settling in water (DeNovio et al., 2004). Colloids in natural subsurface environments include silicate clays, Fe and Al oxides, mineral precipitates, humic materials, and microorganisms (McCarthy and Zachara, 1989). These colloid particles can be released into the soil solution and groundwater through a variety of hydrologic, geochemical, and microbiological processes such as: translocation from the vadose zone (Nyhan et al., 1985), dissolution of minerals and surface coatings (Ryan and Gschwend, 1990), precipitation from solution (Gschwend and Reynolds, 1987), deflocculation of aggregates (McCarthy and Zachara, 1989), microbial-mediated solubilization of humic substances from kerogen and lignitic materials (Ouyang et al., 1996), and land application of raw and treated wastewater (Gerba and Smith, 2005). Consequently, colloid particles vary widely in concentration, composition, structure, and size depending on site-specific properties. Colloid concentrations have typically been reported to range from 10^8 to 10^{17} particles per liter (Kim, 1991). DeNovio et al. (2004) has provided more specific information on colloid concentration ranges in the vadose zone.

An understanding and ability to characterize the transport and retention of colloids in subsurface environments is needed for a wide variety of purposes. For example, the migration of clay particles in porous media is an important process in soil genesis, erosion, and aquifer and petroleum reservoir production because it has a pronounced influence on the ability of porous media to transmit fluids and solutes (Khilar and Fogler, 1998; Mays and Hunt, 2005). Surface water and wastewater treatment processes such as groundwater recharge, riverbank filtration, infiltration ponds and galleries, and sand filtration rely on the efficient removal and inactivation of biocolloids (viruses, bacteria, and protozoan parasites) during passage through porous media (Schijven and Hassanizadeh, 2000; Tufenkji et al., 2002; Ray et al., 2002; Weiss et al., 2005). Many of these biocolloids pose a risk to public health and are therefore contaminants of concern in surface water and drinking water supplies and on agricultural produce (Gerba et al., 1996; Loge et al., 2002; Abbaszadegan et al., 2003). Efficient and cost-efficient design of bioremediation strategies (bioaugmentation and biostimulation) to clean up a variety of recalcitrant chemicals in the subsurface requires knowledge of the transport and fate of bacteria in these environments (Mishra et al., 2001; Vidali, 2001; Gargiulo et al., 2006). Furthermore,

S.A. Bradford, USDA-ARS, U.S. Salinity Lab., 450 W. Big Springs Rd., Riverside, CA 92507; S. Torkzaban, Dep. of Chemical and Environmental Engineering, Univ. of California, Riverside, CA. Received 15 May 2007.
*Corresponding author (sbradford@ussl.ars.usda.gov).

Vadose Zone J. 7:667–681
doi:10.2136/vzj2007.0092

high-surface-area colloids that are mobile can facilitate the transport of many inorganic and organic contaminants that strongly adsorb to the solid phase (Grolimund et al., 1996; Kim et al., 2003; Chen et al., 2005; Šimůnek et al., 2006). Hence, effective treatment processes for many colloids and contaminants relies on the optimization of colloid transport or retention in unsaturated or variably saturated porous media.

Considerable research has been devoted to the fate and transport of colloids in porous media (reviews have been given by Herzig et al., 1970; McDowell-Boyer et al., 1986; McCarthy and Zachara, 1989; Ryan and Elimelech, 1996; Khilar and Fogler, 1998; Schijven and Hassanizadeh, 2000; Harvey and Harms, 2002; Jin and Flury, 2002; Ginn et al., 2002; de Jonge et al., 2004; DeNovio et al., 2004; Rockhold et al., 2004; Sen and Khilar, 2006; Tufenkji et al., 2006). In spite of all of this research attention, the mechanisms of colloid transport and retention in porous media are still incompletely understood and quantified. For example, traditional colloid filtration theory assumes an exponential decrease in colloid retention with transport distance (e.g., Yao et al., 1971; Logan et al., 1995; Tufenkji and Elimelech, 2004). In contrast, under saturated conditions that are unfavorable for attachment (when repulsive electrostatic interactions exist between the colloids and the grain surfaces), retained colloids frequently exhibit a depth-dependent deposition rate that produces hyperexponential (a decreasing rate of deposition coefficient with distance) (Albinger et al., 1994; Baygents et al., 1998; Simoni et al., 1998; Bolster et al., 2000; DeFlaun et al., 1997; Zhang et al., 2001; Redman et al., 2001; Bradford et al., 2002; Li et al., 2004; Bradford and Bettahar, 2005) or nonmonotonic (a peak in retained colloids away from the injection source) (Tong et al., 2005; Bradford et al., 2006b) deposition profiles. Deviations between experimental observations and filtration theory predictions have been reported to increase for larger colloids and finer textured porous media (Bradford et al., 2003; Tufenkji and Elimelech, 2005a) and at larger transport distances (Bolster et al., 2000; Bradford and Bettahar, 2005).

Various hypotheses have been proposed in the literature to account for the observed deviations from filtration theory predictions. Chemical explanations include porous media charge variability (Johnson and Elimelech, 1995), heterogeneity in surface charge characteristics of colloids (Bolster et al., 1999; Li et al., 2004), deposition of colloids in the secondary energy minimum of the Derjaguin–Landau–Verwey–Overbeek (DLVO) interaction energy curve (Redman et al., 2004; Hahn et al., 2004; Tufenkji and Elimelech, 2005a), time-dependent attachment (Tan et al., 1994; Liu et al., 1995), and colloid detachment (Tufenkji et al., 2003). Other researchers have suggested that deposition may occur as a result of physical factors that are not included in filtration theory, such as straining (deposition of colloids in small pore spaces such as those formed at grain–grain contacts) (Cushing and Lawler, 1998; Bradford et al., 2002, 2003, 2004, 2005, 2006a,b; Li et al., 2004; Tufenkji et al., 2004; Bradford and Bettahar, 2005; Foppen et al., 2005), soil surface roughness (Kretzschmar et al., 1997; Redman et al., 2001), and hydrodynamic drag (Li et al., 2005).

Most of the above-cited research pertains to saturated media; less is known about colloid transport and retention in unsaturated systems (Wan and Wilson, 1994b; Choi and Corapcioglu, 1997; Wan and Tokunaga, 1997; Schafer et al., 1998a,b; Saiers et al., 2003; Saiers and Lenhart, 2003; Cherrey et al., 2003; de Jonge et al., 2004; DeNovio et al., 2004; Chen and Flury, 2005). Colloid retention mechanisms in the vadose zone are even more complicated than in the saturated zone, mainly due to the presence of air in the system. In unsaturated porous media, water flow is restricted by capillary forces to the smaller regions of the pore space and flow rates are relatively small. Colloid transport may be influenced by increased attachment to the solid–water interface (SWI) (Chu et al., 2001; Lance and Gerba, 1984; Torkzaban et al., 2006a), attachment to the air–water interface (AWI) (Wan and Wilson, 1994a,b; Schafer et al., 1998a; Cherrey et al., 2003; Torkzaban et al., 2006b), film straining in water films enveloping the solid phase (Wan and Tokunaga, 1997; Saiers and Lenhart, 2003), and retention at the solid–air–water triple point (Chen and Flury, 2005; Crist et al., 2004, 2005; Zevi et al., 2005; Steenhuis et al., 2006). Transients in water content during infiltration and drainage processes can also significantly influence these unsaturated colloid retention mechanisms (Saiers et al., 2003; Saiers and Lenhart, 2003; Torkzaban et al., 2006b).

The above literature indicates that many colloid retention processes are still poorly understood and quantified. To improve our knowledge of colloid fate in unsaturated porous media, this review focuses on physicochemical and hydrodynamic factors that will influence the transport and retention of colloids at the interface, collector, and pore scales. In this work, the interface scale is used to study colloid interactions near a single SWI or AWI that occur across the size range of several colloid diameters. The collector scale is used to study colloid transport and interactions on a single solid grain or air bubble collector, while the pore scale is used to study these processes in pore spaces that are defined by several collectors or multiple interfaces. The study of colloid retention at these small scales provides insight into different mechanisms and factors that influence the transport and fate of colloids at the larger scales that are typically considered in the laboratory and the field. Furthermore, diverse modeling approaches and experimental methodologies are needed to investigate colloid transport and retention processes at the small scale. The main objectives of this work are to: (i) review our current understanding of mechanisms, factors, and models of colloid transport and retention at the interface, collector, and pore scales; (ii) identify gaps in knowledge; and (iii) provide recommendations and illustrative examples of how to tackle these knowledge gaps at the small scale. Biological aspects of colloid retention and fate (growth, inactivation, and degradation) are not considered here. The interested reader is referred to recent reviews on this topic (Baveye et al., 1998; Schijven and Hassanizadeh, 2000; Harvey and Harms, 2002; Jin and Flury, 2002; Ginn et al., 2002; Rockhold et al., 2004; Tufenkji et al., 2006).

Interface Scale

Derjaguin–Landau–Verwey–Overbeek Interactions

The interface scale is well suited for quantifying the interaction energy of a colloid as a function of separation distance from the SWI, the AWI, or other colloids. The interaction energy plays a critical role in determining the potential for colloid attachment to these interfaces, as well as in the stability of colloidal suspensions (Elimelech et al., 1998). Interaction energies have typically been calculated using DLVO theory as the sum of electrostatic

and van der Waals interaction energies (Derjaguin and Landau, 1941; Verwey and Overbeek, 1948):

$$\Phi_{total}(h) = \Phi_{el}(h) + \Phi_{vdW}(h) \quad [1]$$

where Φ_{total} [M L^2 T^{-2}], Φ_{el} [M L^2 T^{-2}], and Φ_{vdW} [M L^2 T^{-2}] are the total, electrostatic, and van der Waals interaction energies, respectively, and h [L] is the separation distance between the colloids and the interface of interest. Values of Φ_{total}, Φ_{el}, and Φ_{vdW} are commonly made dimensionless by dividing by the product of the Boltzmann constant (k_B = 1.38 × 10^{-23} J K^{-1}) and the absolute temperature (T_K).

Expressions for Φ_{el} are available in the literature for different system geometries and assumptions (Elimelech et al., 1998). These expressions were derived from various approximations of the Poisson–Boltzmann equation that accounts for electrostatic interactions of charged bodies in ionic solutions as a result of the overlap of their diffuse double layers. The electrostatic double layer interactions can be determined using the constant surface potential interaction expression of Hogg et al. (1966) for a sphere–sphere interaction as

$$\Phi_{el}(h) = \frac{\pi\varepsilon\varepsilon_o r_c r_{c2}}{(r_c + r_{c2})}\left\{2\phi_1\phi_2 \ln\left[\frac{1+\exp(-\kappa h)}{1-\exp(-\kappa h)}\right] + (\phi_1^2 + \phi_2^2)\ln\left[1-\exp(-2\kappa h)\right]\right\} \quad [2]$$

where ε (dimensionless) is the dielectric constant of the medium, ε_o [M^{-1} L^{-3} T^4 A^{-2}, where A denotes ampere] is the permittivity in a vacuum, r_c [L] is the radius of a colloid, r_{c2} [L] is the radius of the second sphere, ϕ_1 [M L^2 T^{-3} A^{-1}] is the surface potential of the colloid, ϕ_2 [M L^2 T^{-3} A^{-1}] is the surface potential of the second sphere, and κ [L^{-1}] is the Debye–Huckel parameter. The value of κ is inversely related to the thickness of the diffuse double layer thickness and is given as

$$\kappa = \sqrt{\frac{1000 e^2 N_A}{\varepsilon k_B T_K}\sum_i M_i z_i^2} \quad [3]$$

where N_A is Avagadro's number (6.02 × 10^{23} molecules mole^{-1}), M_i is the molar concentration of the electrolyte (mol L^{-1}), e is the charge of an electron (1.602 × 10^{-19} C), and z (dimensionless) is the valence of the electrolyte. The colloid-collector system is frequently treated as a sphere–plate interaction, and a similar expression is obtained from Eq. [2] by taking the limit as r_{c2} goes to infinity. In this case, the quantity $(r_c r_{c2})/(r_c + r_{c2})$ is replaced by r_c.

Measured zeta potentials are frequently used in place of surface potentials in Eq. [2]. Zeta potentials for clean quartz and glass typically range from around –10 to –80 mV depending on the solution chemistry (Elimelech and O'Melia, 1990; Elimelech et al., 2000; Redman et al., 2004). The AWI has also been reported to be negatively charged (Ducker et al., 1994; Wan and Wilson, 1994a; Kelsall et al., 1996; Abdel-Fattah and El-Genk, 1998; Chen and Flury, 2005; Saiers and Lenhart, 2003; Lazouskaya et al., 2006), and reported measurements range from around –15 to –65 mV. In the calculations presented below, the zeta potentials for quartz and the AWI were assumed to be –20 and –50 mV, respectively.

The van der Waals interactions also exist between colloids in suspension and charged surfaces due to the presence of intermolecular forces that occur as a result of polarization of molecules into dipoles. Various expressions for Φ_{vdW} have been summarized by Elimelech et al. (1998). For sphere–sphere interactions, the retarded van der Waals interaction energy, Φ_{vdW}, can be determined using the expression by Gregory (1981) as

$$\Phi_{vdW}(h) = -\frac{A_{123} r_c r_{c2}}{6h(r_c + r_{c2})}\left[1 + \frac{14h}{\lambda}\right]^{-1} \quad [4]$$

where A_{123} [M L^2 T^{-2}] is the Hamaker constant in this system, and λ [L] is the characteristic wavelength that is often taken as 100 nm (Gregory, 1981). When the colloid-collector system is treated as a sphere–plate interaction, the quantity $(r_c r_{c2})/(r_c + r_{c2})$ in Eq. [4] is replaced by r_c.

The value of the Hamaker constant that is required in Eq. [4] is typically estimated from the following expression (Israelachvili, 1992):

$$A_{123} = \left(\sqrt{A_{11}} - \sqrt{A_{33}}\right)\left(\sqrt{A_{22}} - \sqrt{A_{33}}\right) \quad [5]$$

where A_{11} [M L^2 T^{-2}] is the Hamaker constant of the colloid, A_{22} [M L^2 T^{-2}] is the Hamaker constant for the collector surface, and A_{33} [M L^2 T^{-2}] is the Hamaker constant for the aqueous solution. The values of the Hamaker constant for polystyrene latex, glass, quartz, water, and air are reported to be 6.6 × 10^{-20}, 6.34 × 10^{-20}, 6.5 × 10^{-20}, 3.7 × 10^{-20} J, and zero, respectively (Israelachvili, 1992). Hence, attractive van der Waals interaction occurs on glass and quartz surfaces and the value of A_{123} is equal to 3.79 × 10^{-21} J for polystyrene–water–glass systems, and 4.04 × 10^{-21} J for polystyrene–water–quartz systems. In contrast, the value of A_{123} for polystyrene–air–water systems is equal to –1.2 × 10^{-20} J (Israelachvili, 1992), implying that the van der Waals interaction is repulsive for polystyrene colloids at the AWI.

The DLVO theory discussed above has proven to be a useful tool to explore the influence of solution and interface chemistry and colloid size on colloid attachment to various interfaces. Figure 1 presents plots of the calculated total DLVO interaction energy profiles for the 1- and 3-μm polystyrene latex microsphere colloids in 10 and 100 mmol L^{-1} ionic strength solution on approach to a quartz surface (Fig. 1a) and the AWI (Fig. 1b). In these calculations, literature values for the zeta potential of 1- and 3-μm colloids were assumed to be –77 and –57 mV (Bradford et al., 2002), respectively. The DLVO calculations revealed the presence of a significant energy barrier to attachment in the primary minimum on quartz and the AWI at both ionic strengths of 10 and 100 mmol L^{-1}. Under these chemically unfavorable attachment conditions, the DVLO calculations predict that colloids can still interact with quartz due to the presence of a secondary energy minimum at separation distances greater than the location of the energy barrier (the depth of the secondary minimum for the 1- and 3-μm colloids was equal to –0.4 and –1.4 $k_B T_K$ when the ionic strength was 10 mmol L^{-1}, and was –4.8 and –15.5 $k_B T_K$ when the ionic strength was 100 mmol L^{-1}, respectively). The depth of the secondary energy minimum increased with colloid size and ionic strength due to an enhancement in attractive van der Waals interactions and compression in double layer thickness. In contrast, DLVO calculations predict that colloids at the AWI

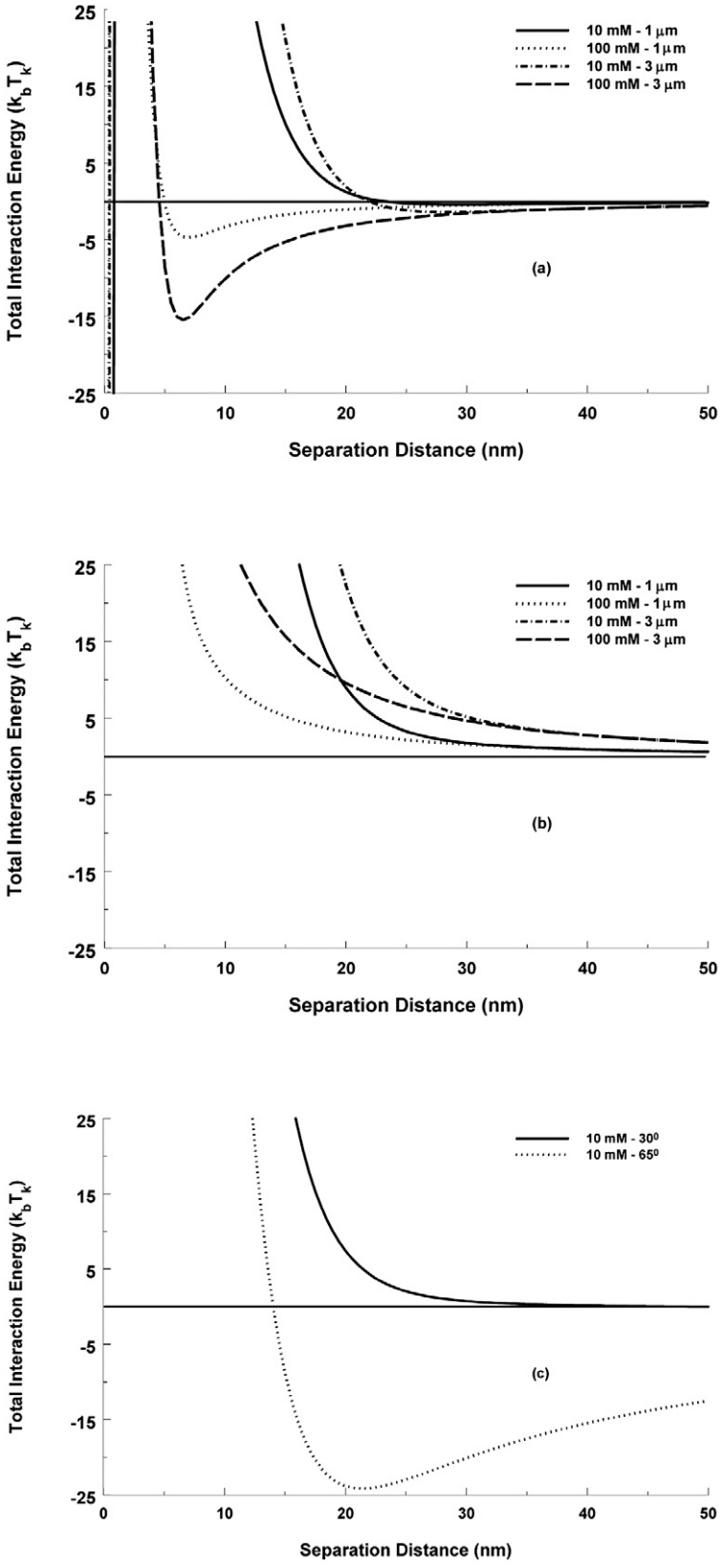

FIG. 1. Plots of the calculated total interaction energy profiles when using standard Derjaguin–Landau–Verwey–Overbeek (DLVO) theory for the 1- and 3-μm polystyrene latex microsphere colloids in 10 and 100 mmol L^{-1} ionic strength solution on approach to (a) a quartz surface and (b) the air–water interface (AWI); (c) a similar plot when using extended DLVO theory that considers hydrophobic interactions (Eq. [2], [4], [6], [9], and [10]) for colloids on approach to the AWI when the suspension ionic strength was 10 mmol L^{-1} and the colloid contact angle was equal to 30 and 65°.

experience repulsive electrostatic and van der Waals interactions and therefore do not interact with the AWI. Indeed, Wan and Tokunaga (2002) demonstrated in bubble column experiments that only positively charged colloids attached to the negatively charged AWI.

Hydrophobic and Capillary Forces

The DLVO theory does not accurately describe all colloid interactions on SWI and, especially, AWI and other colloid interfaces (van Oss et al., 1988; Grasso et al., 2002; Lazouskaya et al., 2006). Non-DLVO interactions that may occur at these interfaces have been reviewed by Grasso et al. (2002) and include H bonding, hydrophobic interactions, hydration pressure, non-charge-transfer Lewis acid–base interactions, and steric interactions. Many of these non-DLVO interactions are still incompletely understood and quantitative theory has not been generally accepted to describe such interactions.

In unsaturated systems, hydrophobic interactions of colloids at the AWI may play a potentially significant role in colloid attachment (Schafer et al., 1998a,b; Lazouskaya et al., 2006; Johnson et al., 2006). Colloid stability and aggregation is also reported to be sensitive to the surface hydrophobicity (Crist et al., 2005; Breiner et al., 2006). The DLVO theory can be extended to include the potential influence of hydrophobic interactions on attachment as

$$\Phi_{\text{total}}(h) = \Phi_{\text{el}}(h) + \Phi_{\text{vdW}}(h) + \Phi_{\text{Hyd}}(h) \quad [6]$$

where Φ_{Hyd} [M L^2 T^{-2}] is the interaction energy due to hydrophobic effects.

Van Oss (1994) has proposed a mechanistic model for the calculation of hydrophobic interactions that is based on the Lewis acid–base free energy of adhesion. In brief, the Lewis acid–base interaction energy between a spherical colloid and a flat solid surface is given as (van Oss, 1994)

$$\Phi_{\text{Hyd}}(h) = 2\pi r_c \lambda_{\text{AB}} \Delta\Phi_{d_o}^{\text{AB}} \exp\left(\frac{d_o - h}{\lambda_{\text{AB}}}\right) \quad [7]$$

where λ_{AB} [L] is the water decay length for acid–base interactions that is typically accepted to be around 1 to 2 nm (Israelachvili, 1992), and d_o [L] is the distance of closest approach where physical contact occurs between the colloid and the solid surface and is assumed to be 0.158 nm (van Oss, 1994). The parameter $\Delta\Phi_{d_o}^{\text{AB}}$ [M T^{-2}] is the free energy of adhesion at d_o and is given as (van Oss, 1994)

$$\Delta\Phi_{d_o}^{\text{AB}} = 2\left[\sqrt{\gamma_w^+}\left(\sqrt{\gamma_c^-} + \sqrt{\gamma_s^-} - \sqrt{\gamma_w^-}\right) + \sqrt{\gamma_w^-}\left(\sqrt{\gamma_c^+} + \sqrt{\gamma_s^+} - \sqrt{\gamma_w^+}\right) - \sqrt{\gamma_c^+\gamma_s^-} - \sqrt{\gamma_c^-\gamma_s^+}\right] \quad [8]$$

where γ_w^+ [M T^{-2}], γ_s^+ [M T^{-2}], γ_c^+ [M T^{-2}], γ_w^- [M T^{-2}], γ_s^- [M T^{-2}], and γ_c^- [M T^{-2}] are the Lewis acid (superscript +) and base (superscript –) surface components of water (subscript w), solid (subscript s), and colloid (subscript c). Values of γ_w^+ and γ_w^- are reported to be 25.5 and 25.5 mJ m^{-2}, respectively (van Oss, 1994). Bergendahl and Grasso (1999) reported that γ_c^+ and γ_c^- for polystyrene latex was 0 and 5.9 mJ m^{-2}, respectively. These same

researchers reported that γ_s^+ and γ_s^- for glass was sensitive to the surface preparation, with γ_s^+ ranging from 0.4 to 2.3 mJ m^{-2} and γ_s^- from 26.2 to 62.2 mJ m^{-2}. Chen and Flury (2005) reported for various clays that γ_s^+ ranged from 0.0 to 1.1 mJ m^{-2} and γ_s^- from 27.5 to 44.5 mJ m^{-2}. It should be mentioned that values of γ_s^+, γ_s^-, γ_c^+ and γ_c^- are functions of their surface hydrophobicity, and that these parameters can be determined using measured contact angles and interfacial tension in several different fluids in conjunction with the Young–Dupre equation (e.g, Bergendahl and Grasso, 1999). To estimate Lewis acid–base interactions for colloids at the AWI, the values of γ_s^+ and γ_s^- in Eq. [8] need to be replaced by γ_a^+ and γ_a^- for the air phase. Values of γ_a^+ and γ_a^- have both been reported to be equal to zero (van Oss, 2006).

Disagreement about the origins of hydrophobic interactions, however, still prevails (Tsao et al., 1993, Yaminsky and Ninham, 1993; Rabinovich and Yoon, 1994; van Oss, 1994; Yoon and Ravishankar, 1996). Alternatively, asymmetric hydrophobic interactions between two surfaces can be calculated based on their contact angles (Yoon et al., 1997; Schafer et al., 1998a). The following empirical expression has been proposed to quantify this interaction as a function of separation distance for sphere–plate systems as (Schafer et al., 1998a)

$$\Phi_{\mathrm{Hyd}}(h) = -\frac{K_{123} r_c}{h} \qquad [9]$$

where K_{123} [M L^2 T^{-2}] is the force constant for the asymmetric interactions between macroscopic bodies 1 and 2 in medium 3. The value of K_{123} has been determined as (Yoon et al., 1997; Schafer et al., 1998a)

$$\log K_{123} = a\left(\frac{\cos\theta_c + \cos\theta_2}{2}\right) + b \qquad [10]$$

where θ_c (°) is the contact angle on a colloid surface, and θ_2 (°) is the contact angle on a second surface, and a and b (both dimensionless) are system-specific constants. For the illustrative examples presented below, we assumed that colloids had a value of θ_c equal to 30 and 65°, respectively. We also assumed that clean quartz or glass surfaces had θ_2 equal to 0°, and the value of θ_2 at the air surface is equal to 180° (Schafer et al., 1998a; van Oss, 2006). Values of a = –6 and b = –22 were taken from Crist et al. (2005).

Equation [10] indicates that hydrophobic interactions will be much greater on the AWI than on the quartz–water interface because of the pronounced difference in θ_2 (0 vs. 180°). As an illustration of the potential significance of hydrophobic interactions on colloid attachment to the AWI, Fig. 1c presents a plot of the total extended DLVO interaction energy on approach of 1-μm polystyrene latex microspheres to the AWI when the suspension ionic strength was 10 mmol L^{-1} and θ_c was equal to 30 and 65°. It can be observed that colloids with θ_c = 65° exhibit much greater affinity for the AWI than the θ_c = 30° colloids.

When the colloid enters into the AWI, a capillary force (F_{Cap}) will also act on the attached colloids. The vertical component of the capillary force that acts on a colloid at the AWI is given as (Zhang et al., 1996; Veerapaneni et al., 2000):

$$F_{\mathrm{Cap}} = 2\pi x_c \sigma \sin(\phi_c) + \pi x_c^2 \Delta P_e \qquad [11]$$

where σ [M T^{-2}] is the surface tension of water, x_c [L] is the horizontial distance measured from the axis of symmetry to the contact point of the AWI on the colloid surface, ϕ_c (°) is the angular inclination of the AWI interface to the horizontal at its line of contact with the colloid, and ΔP_e [M L^{-1} T^{-2}] is the excess pressure that acts on the colloid and is proportional to the height of the capillary rise on the colloid surface. For colloids with a hydrophobic surface, the capillary force will be dominated by the surface tension force (the first term on the right-hand side of Eq. [11]) (e.g., Johnson et al., 2006). The capillary force will only play a significant factor in attachment to the AWI once the colloids enter the interface, i.e., when the energy barrier to attachment has been overcome. In contrast to the SWI, the position of the AWI moves during wetting and drainage cycles. It has been postulated that movement of the AWI during water drainage could potentially capture colloids attached on the SWI by capillary forces (Saiers et al., 2003; Saiers and Lenhart, 2003; Torkzaban et al., 2006a).

Colloid Attachment and Detachment

For attachment to occur, the net adhesive force or torque acting on colloids in the vicinity of an interface must overcome the hydrodynamic forces and the applied torque. To obtain the adhesive force acting on colloids in the proximity of an interface in terms of the calculated interaction energy, the Derjaguin and Langbein approximations can be used (Israelachvili, 1992). Specifically, the value of the adhesive force (F_A) is estimated as Φ_{min}/h, where Φ_{min} [M L T^{-2}] is the absolute value of the secondary or primary minimum interaction energy. The adhesive or resisting torque (T_{adhesive} [M L^2 T^{-2}]) for colloids attached in either the secondary or primary minimum is represented by the net adhesive force (F_A) acting on a lever arm (l_x [L]) as

$$T_{\mathrm{adhesive}} = F_A l_x \qquad [12]$$

The value of F_A corresponds to the extended-DLVO force of adhesion, which must be overcome to detach the particle from the secondary or primary energy minimum. On smooth surfaces, the value of l_x is provided by the radius of the colloid–surface contact area that was estimated using the approach of Johnson et al. (1971). Since there is no direct physical contact between colloids attached in the secondary minimum and the interface, the corresponding contact radius is given as (Israelachvili, 1992)

$$l_x = \left(\frac{F_A r_c}{4K}\right)^{1/3} \qquad [13]$$

where K [M L^{-1} T^{-2}] is the composite Young's modulus (Johnson et al., 1971). Bergendahl and Grasso (2000) used a value of K = 4.014×10^9 N m^{-2} for glass bead collectors and a polystyrene colloid suspension.

Hydrodynamic forces also act on colloids that are in the vicinity of the SWI or AWI as a result of water flow. When the water flow is laminar, the lift force acting on the colloid perpendicular to the interface is negligible (Soltani and Ahmadi, 1994) and the drag force that acts on the colloid tangential to the interface is significant and can be determined using the following equation (Goldman et al., 1967; O'Neill, 1968):

$$F_D = 10.205\pi\mu(\partial V/\partial r)r_c^2 \quad [14]$$

where $\partial V/\partial r$ [T^{-1}] is the hydrodynamic shear at a distance of r_c from the surface, and μ [M L^{-1} T^{-1}] is the fluid dynamic viscosity.

A colloid that collides with an interface may not succeed in attachment or the previously attached colloids may detach from the interface. Lifting, sliding, and rolling are the hydrodynamic mechanisms that can cause colloid removal from an interface (Soltani and Ahmadi, 1994; Bergendahl and Grasso, 2000). Rolling has been reported to be the dominant mechanism of detachment from solid surfaces under laminar flow conditions (Tsai et al., 1991; Bergendahl and Grasso, 1998, 1999). Rolling occurs when the adhesive torque—the resistance to rolling—is overcome by the applied torque ($T_{applied}$ [M L^2 T^{-2}]) from hydrodynamic forces (Johnson, 1985). The applied torque acting on the colloid in the vicinity of the solid interface due to the hydrodynamic shear force is given as (Goldman et al., 1967; O'Neill, 1968)

$$T_{applied} = 1.4 r_c F_D \quad [15]$$

Due to the increase in velocity with distance from the interface, the drag force effectively acts on the attached particle at a height of $1.4r_c$; thus, the drag force creates a torque by acting on a lever arm of $1.4r_c$ (Goldman et al., 1967; O'Neill, 1968).

In the above analysis of torques, a smooth interface and colloid were assumed. In this case, a single adhesion force reasonably describes the interaction (Burdick et al., 2005). The lever arms that act on the adhesive and applied torques, however, have been reported to be a strong function of the surface roughness of the interface and the colloid (Hubbe, 1984; Das et al., 1994; Burdick et al., 2005). Burdick et al. (2005) reported that the lever arm for the applied torque decreased with increasing size of surface roughness and was zero when the roughness was greater than the colloid radius. Conversely, the lever arm that acted on the adhesive torque was reported to increase with increasing size of the surface roughness. Hence, when the interface or the colloid was rough, a distribution of adhesion forces was obtained (Cooper et al., 2000a,b, 2001). Hoek and Agarwal (2006) reported that colloids in the immediate vicinity of multiple SWIs experience greater DLVO forces than colloids on a single SWI. All of these factors indicate that greater retention of colloids is expected on rough than on smooth interfaces.

The information presented above indicates that colloid attachment and detachment will be dependent on the hydrodynamic and adhesive forces. Published literature (Ryan and Elimelech, 1996) also suggests that the diffusion force will play a role in these processes. Brownian motion of colloids in suspension (diffusion) occurs as a result of fluctuations in the number of collisions between the fluid molecules and the colloids. The Brownian diffusion force (F_B) has been modeled as a Gaussian white noise process as (Gupta and Peters, 1985; Ahmadi and Chen, 1998; Kim and Zydney, 2004)

$$F_B(t) = U(t)\sqrt{\frac{12\pi r_c \mu k_B T_K}{\Delta t}} \quad [16]$$

where $U(t)$ (dimensionless) is a function that generates random numbers between –0.5 and 0.5, and t [T] denotes time. In the limit as time goes to infinity, the distribution of energies that are associated with diffusing colloids in suspension will approach a Maxwellian distribution (Chandrasekhar, 1943). In this case, the fraction of diffusing colloid particles ($f_{\Phi 1}$) that possess energy less than a given dimensionless energy (divided by $k_B T_K$) of Φ_1 is given as (e.g., Simoni et al., 1998)

$$f_{\Phi 1} = \int_0^{\Phi_1} \frac{2}{k_B T_K}\left(\frac{E}{\pi k_B T_K}\right)^{0.5} \exp\left(-\frac{E}{k_B T_K}\right) dE = \frac{\Gamma_i(1.5, \Phi_1)}{\Gamma(1.5)} \quad [17]$$

where E [M L^2 T^{-2}] is the kinetic energy of diffusing colloids, Γ_i is the incomplete gamma function, and Γ is the gamma function. Simoni et al. (1998) and Dong et al. (2002) have used Eq. [17] under unfavorable attachment conditions to estimate the fraction of colloids colliding with the solid surface that can be attached by setting Φ_1 to the absolute magnitude of the depth of the secondary energy minimum. Conversely, this analysis implies that the complementary fraction of colloids that collide with the solid surface, $1 - f_{\Phi 1}$, would detach from the solid surface via diffusion. This analysis, however, neglects the potential influence of hydrodynamic forces on colloid detachment.

Collector Scale

At the collector scale, the aqueous flow field can be solved and the rate of mass transfer to a simple collector surface can be calculated. The water flow field around a solid grain or an air bubble spherical collector can be found from the solution of the Navier–Stokes equations:

$$\rho\left(\frac{\partial \mathbf{v}}{\partial t} + \mathbf{v} \bullet \nabla \mathbf{v}\right) = -\nabla p + \mu \nabla^2 \mathbf{v} + \rho \mathbf{g} \quad [18]$$

where ρ [M L^{-3}] is the fluid density, $\mathbf{v}$ [L T^{-1}] is the velocity vector, p [M L^{-1} T^{-2}] is pressure, and $\mathbf{g}$ [L T^{-2}] is the acceleration due to gravity vector. In filtration theory, a simplified version of Eq. [18] was solved analytically (Yao et al., 1971; Rajagopalan and Tien, 1976). In this work, we solved the Navier–Stokes equation under laminar flow conditions in an axisymmetrical coordinate system using the COMSOL commercial software package (COMSOL, Palo Alto, CA); i.e., under steady-state laminar flow conditions the left-hand side of Eq. [18] is zero. The normal velocity and tangential stress at the side boundaries of the cell around the collector were set equal to zero. Normal pressure differences between the inlet and outlet of the cell were assumed to achieve a range of pore water velocities. A no-slip boundary condition was imposed along the collector surface for a solid grain collector. Since the viscosity of air is much less than that of water, the tangential component of the viscous force at the AWI vanishes (Bird et al., 2002) and there is no momentum transfer (a perfect slip boundary condition):

$$\nabla \mathbf{v} \bullet \mathbf{t} = 0 \quad [19]$$

where $\mathbf{t}$ is the tangential unit vector at the AWI. It should be mentioned that other boundary conditions have been applied to the AWI (Lazouskaya et al., 2006). Partial-slip boundary conditions are likely to be more physically realistic when surface-active impurities accumulate at the AWI.

Figure 2 presents a plot of the velocity distribution at a distance of 0.5 μm from the surface of 400-μm spherical grain and air bubble collectors when the average pore water velocity was 1 m d^{-1}. Using Eq. [14], this velocity information can be used to calculate the distribution of drag forces that acts on 1-μm colloids that are attached to these collector surfaces. Notice that higher velocities occur on the sides of the collectors that are parallel to the flowing water, and zones of relative flow stagnation occur at the top (front stagnation point occurs at $L/L_{max} = 0$) and bottom (rear stagnation point occurs at $L/L_{max} = 1$) of the collectors that are perpendicular to flowing water. For a given average pore water velocity, the solid collector has lower velocities near the collector surface than the air bubble. This occurs because of the no-slip boundary condition on the solid grain collector surface (i.e., the velocity at the SWI is zero).

Colloid attachment under saturated conditions is commonly described by colloid filtration theory, originally developed by Yao et al. (1971). According to this theory, the attachment rate coefficient is dependent on the mass transfer of colloids to the collector surface and subsequent colloid–surface interactions. The sphere-in-cell model was used in filtration theory (Happel, 1958; Payatakes et al., 1974) to study colloid mass transfer due to interception, sedimentation, and diffusion to a single spherical solid collector. At the column scale, filtration theory preserves the overall porosity by representing the liquid as a continuous sheath completely surrounding the collector grains of a porous medium. Under unfavorable attachment conditions, the attachment coefficient (k_{att} [T^{-1}]) is given by filtration theory as

$$k_{att} = \frac{3(1-\theta)}{2d_{50}}\alpha\eta v_{avg} \qquad [20]$$

Here v_{avg} [$L\ T^{-1}$] is the average pore water velocity, d_{50} [L] is the median grain diameter, θ (dimensionless) is the volumetric water content, η (dimensionless) is the collector efficiency, and α (dimensionless) is the collision or sticking efficiency. It should be mentioned that filtration theory was originally developed for favorable attachment conditions and in this case α = 1 in Eq. [20].

The parameter η in Eq. [20] accounts for the mass flux of colloids to the collector surface via diffusion, interception, and sedimentation and is defined as the ratio of the integral of the colloid flux that strikes the collector to the rate at which particles flow toward the collector (Yao et al., 1971). The parameter η has been extensively studied for ideal systems, composed of a spherical collector with a smooth surface. Assuming a perfect sink at the collector boundary, the advection–diffusion equation is used to quantify mass transfer to the collector surface in the sphere-in-cell model as (e.g., Ryan and Elimelech, 1996)

$$\frac{\partial C}{\partial t} = \nabla\bullet(\mathbf{D}\bullet\nabla C) - \nabla\bullet(\mathbf{v}C) - \nabla\bullet\left(\frac{\mathbf{D}\bullet\mathbf{F}}{k_B T_K}C\right) \qquad [21]$$

where C [$N_c\ L^{-3}$, where N_c denotes the number of colloids] is the aqueous colloid concentration, $\mathbf{D}$ [$L^2\ T^{-1}$] is the colloid diffusion tensor, and $\mathbf{F}$ [$M\ L\ T^{-2}$] is the external force vector. The first, second, and third terms on the right-hand side of Eq. [21] account for the colloid flux due to diffusion, advection, and external forces (e.g., gravity and adhesive forces), respectively. Correlation equations to predict η as a function of system variables have been developed from simulation results (Rajagopalan and Tien, 1976; Tufenkji and Elimelech, 2004). More recently, the sensitivity of η to variations in collector shape and roughness was found to be significant (Saiers and Ryan, 2005). It should be mentioned, however, that these correlations are only explicitly valid for saturated systems.

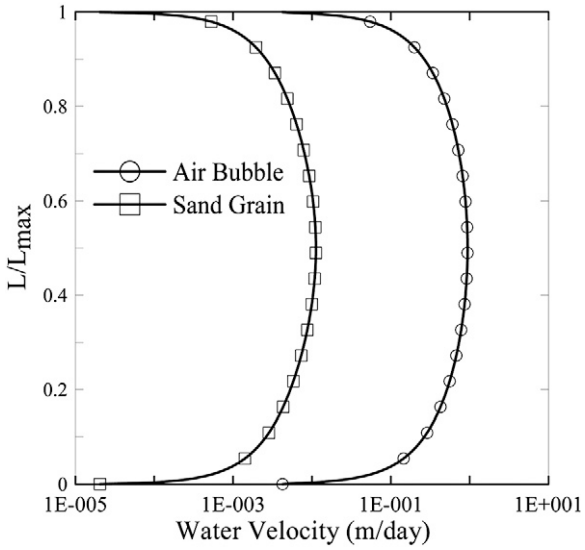

FIG. 2. The calculated distribution of water velocity at a distance of 0.5 μm from the surface of 400-μm spherical solid and air bubble collectors when the average pore water velocity was 1 m d^{-1}. The distribution of water velocity along the collector surface is plotted vs. normalized distance (L/L_{max}), which is defined as the distance from the front toward the rear stagnation point (L) divided by the distance between the front and rear stagnation points (L_{max} = π times the radius of the collector).

Colloid filtration theory originally assumed that colloids were irreversibly retained in the primary minimum of the DLVO interaction energy distribution (Ryan and Elimelech, 1996). In this case, physicochemical forces between colloids and collectors will determine the probability of the success in colloid attachment once they collide with the collector surface (Ryan and Elimelech, 1996), i.e., the value of α in Eq. [20]. Differences in mineralogy and the presence of coatings of metal oxides or organic matter are expected to produce variations in surface charge (Davis, 1982; Tipping and Cooke, 1982; Song and Elimelech, 1993, 1994). In chemically heterogeneous porous media, it is possible to have localized regions that are favorable for attachment and the value of α is therefore proportional to the fraction of the solid surface area that is "favorable" for attachment (Elimelech et al., 2000; Abudalo et al., 2005). Johnson and Li (2005) demonstrated that porous media charge variability and the influence of the DLVO secondary energy minimum should theoretically be consistent with an exponential deposition profile.

A growing body of evidence suggests that attachment in the secondary minimum can significantly contribute to the retention of colloids in saturated porous media (Franchi and O'Melia, 2003; Redman et al., 2004; Hahn and O'Melia 2004; Hahn et al., 2004; Tufenkji and Elimelech, 2005a). Colloids that are attached in the secondary minimum are only weakly associated with the solid phase. In this case, the value of α has been related to the energy of the diffusing colloids and the depth of the secondary minimum according to Eq. [17] when $\alpha = f_{\Phi 1}$ (Simoni et al., 1998; Dong et al., 2002). Recent experimental (Tong et al., 2005; Li and Johnson, 2005; Johnson et al., 2007a) and

theoretical (Torkzaban et al., 2007) evidence also demonstrates that the value of α decreases with increasing water velocity under unfavorable attachment conditions. Furthermore, it has been observed that colloids captured in the secondary energy minimum can be translated along the collector surface via hydrodynamic forces (Kuznar and Elimelech, 2007).

Torkzaban et al. (2007) examined the influence of hydrodynamic and adhesive forces and torques, discussed above, on colloid attachment to glass spheroidal (spheres and ellipsoids) collectors. Figure 3 presents a plot of the fraction of the grain collector surface area (S_f) where attachment may occur ($T_{adhesion} > T_{applied}$) for 1-μm colloids as a function of F_A at several pore water velocities. Notice that on a glass collector, S_f is close to zero at the lowest values of F_A because $T_{adhesion} < T_{applied}$ across the vast majority of the collector surface. As F_A increases, the value of S_f increases to values between 0 and 1. In this case, partially favorable attachment conditions occur. This implies that attachment occurs on regions adjacent to the front and rear stagnation point (i.e., $T_{adhesion} > T_{applied}$), but that conditions are unfavorable for attachment near the collector center because $T_{adhesion} < T_{applied}$. Eventually a value of F_A occurs when S_f is equal to 1 because $T_{adhesion} > T_{applied}$ across the entire collector surface. Increasing the pore water velocity tends to shift these curves to the right because of the higher value of $T_{applied}$. Torkzaban et al. (2007) also found that the value of S_f was a function of collector size and shape. For the same pore water velocity, smaller collectors exhibited smaller values of S_f than larger collectors due to the presence of greater values of $T_{applied}$ near the collector surface. The collector shape also affected the distribution of $T_{applied}$ around the collector surface and therefore S_f.

The above analysis suggests that "partially favorable attachment conditions" may occur when considering both adhesive and hydrodynamic forces. Colloids that collide with the collector surface near the center of the collector may roll on the collector surface and be retained near the rear stagnation point. This result has important implications for the determination of α in these regions, as well as for the time-dependent attachment processes of blocking and ripening. The value of α is expect to be a function of both adhesive and hydrodynamic forces, and to be proportional to S_f. *Blocking* commonly refers to a decreasing rate of attachment as chemically favorable attachment locations are filled (Adamczyk et al., 1994). The above analysis implies that blocking will also depend on the hydrodynamics and adhesive forces of the system that determine S_f. *Ripening* refers to an increasing rate of colloid attachment with time due to colloid–colloid interactions on the collector surface. The role of hydrodynamic forces on colloid ripening have not yet been quantified, but recent experimental data suggests that it could enhance ripening behavior (Bradford et al., 2006b, 2007).

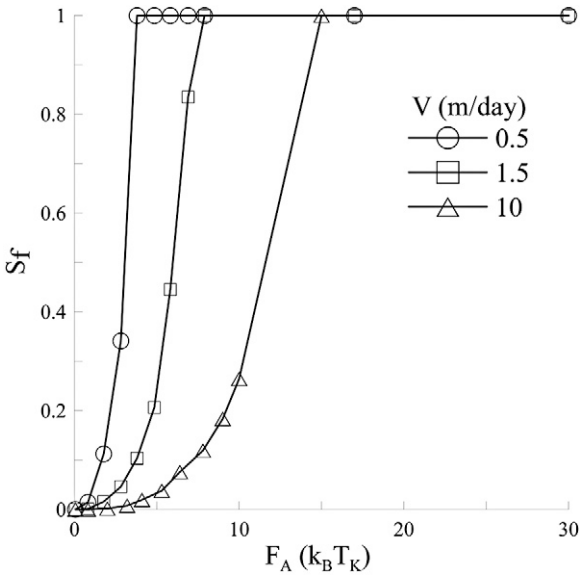

FIG. 3. Plots of the fraction of the grain collector surface area that is favorable for attachment (S_f) for 1-μm colloids as a function of the adhesive force (F_A) at several pore water velocities (0.5, 1.0, and 10.0 m d^{-1}).

Under unfavorable attachment conditions, the hypothesis of colloid charge variability has frequently been invoked to explain experimental deposition profiles for a variety of colloids, including microorganisms (Simoni et al., 1998) and latex microspheres (Li et al., 2004; Tufenkji and Elimelech, 2005b; Tong and Johnson, 2007). Figure 3 can also be used to study the influence of surface charge heterogeneity of colloids or porous media on colloid attachment to a single collector. Surface charge heterogeneity of the colloid and the collector will both influence F_A of colloids that collide with the collector surface. If the zeta potential distributions of either the collector or the colloid is known or assumed, it is possible to determine the fraction of the surface area that is accessible for attachment for a given solution chemistry when the charge heterogeneity (colloid or collector) is uniformly distributed across the collector surface into N categories. In this case, the value of S_f can be determined as

$$S_f = \sum_{i=1}^{N} S_i f_i \qquad [22]$$

where i is the category index, S_i (dimensionless) is the value of S_f for the ith category, and f_i (dimensionless) is the charge heterogeneity fraction of the ith category. When $N = 2$, this approach is similar to that applied in chemically heterogeneous porous media to determine an effective value of α (Elimelech et al., 2000; Abudalo et al., 2005). It should be mentioned, however, that when colloid surface charge variability is considered, the variance in the zeta potential distribution will change with transport distance and result in a decreasing attachment rate coefficient (Bradford and Toride, 2007). In this case, the value of f_i will also change with transport distance. In contrast, heterogeneity in the collector surface charge will not produce any change in the average attachment rate coefficient with transport distance (Johnson and Li, 2005).

The coupled roles of hydrodynamic and adhesive forces on colloid attachment to a spherical air-bubble collector may also be studied by considering the forces and torques that act on the attached colloids. For negatively charged colloids, hydrophobic and capillary forces are expected to play the dominant role in colloid attachment to an air bubble because both electrostatic and van der Waals interactions are repulsive (Fig. 1b). An additional complication arises at the AWI compared with the SWI due to the difference in boundary conditions. Figure 2 indicates that much higher velocities are possible at the AWI than the SWI. The type of boundary condition at the AWI (zero tangential momentum transfer at the interface) dictates that attached colloids are likely to experience a uniform drag force with distance from the

interface, and therefore no applied torque due to hydrodynamic shear. In this case, sliding of colloids at the AWI is possible when (Bergendahl and Grasso, 1998)

$$F_A < \frac{4\left(F_D/\mu_f + F_L\right)}{3} \quad [23]$$

where F_L [M L T^{-2}] is the lift force and μ_f (dimensionless) is the coefficient of sliding friction. Saffman (1965) provided a formula for calculating the lift force near the SWI, but this expression may not be applicable near the AWI due to the different boundary condition. When colloids are attached to the AWI, the value of μ_f is likely to be very small. We are not aware of any published values for μ_f adjacent to the AWI. If a value of μ_f equal to zero is assumed, then Eq. [23] predicts that colloids attached to the AWI will slide along the interface as a result of fluid drag, regardless of the magnitude of F_A. Additional research is warranted to study sliding of attached colloids at the AWI and to determine μ_f.

Pore Scale

The pore scale consists of an ensemble of collectors and differs from the collector scale due to the presence of multiple SWI or AWI and contact points (grain–grain contacts and solid–water–air triple points) that makeup the pore space geometry. The aqueous flow field, mass transfer rate, and forces and torques that act on colloids can also be determined at the pore scale. Differences in pore- and collector-scale variables occur as a result of the pore space geometry. The pore scale is well suited for determining mechanisms of colloid retention in porous media. Indeed, studies have recently examined colloid transport and deposition processes at the pore scale using a variety of techniques (Ochiai et al., 2006). This research has provided valuable insight on colloid retention at the AWI and solid–water–air triple point (Wan and Wilson, 1994a; Sirivithayapakorn and Keller, 2003b; Crist et al., 2004, 2005; Wan and Tokunaga, 2005; Steenhuis et al., 2005), colloid size exclusion (Sirivithayapakorn and Keller, 2003a), colloid dispersion (Auset and Keller, 2004), and attachment and straining processes of colloid retention (Bradford et al., 2005, 2006a,b; Xu et al., 2006; Li et al., 2006; Yoon et al., 2006; Kuznar and Elimelech, 2007).

The geometry presented in Fig. 4 allows a first approximation to mechanistically study the influence of pore structure on colloid transport and retention. Similar geometries have been used by other researchers (Lenormand et al., 1983; Mason and Morrow, 1984, 1991; Li and Wardlaw, 1986; Tuller et al., 1999) to study unsaturated flow. The shape of the AWI at a given capillary pressure can be determined using the Young–Laplace equation:

$$\rho g\psi = \sigma\left(\frac{1}{R_1} + \frac{1}{R_2}\right) \quad [24]$$

where R_1 [L] and R_2 [L] are the principal radii of curvature of the interface, ψ [L] is the matric potential head, and g [L T^{-2}] is the constant of gravitational acceleration. For a spherical interface, $R_1 = R_2$, whereas when R_2 is large, the second term on the right-hand side of Eq. [24] approaches zero. Tuller et al. (1999) has provided relationships to determine the saturation that corresponds to a given interface curvature.

For unsaturated conditions, the equilibrium thickness of the water films at a given capillary pressure can be estimated using the Hamaker equation (Iwamatsu and Horii, 1996):

$$w = \sqrt[3]{\frac{A_{saw}}{6\pi\rho g\psi}} \quad [25]$$

where w [L] is the thickness of the water films, and A_{saw} [M L^2 T^{-2}] is the Hamaker constant for the solid–air–water system. It should be mentioned that even under relatively moist conditions (ψ equal to –5 to –10 cm), the calculated thickness of the water film is around 20 nm. This thickness is much smaller than the size of colloids that are typically used in transport experiments. Under variably saturated flow conditions, equilibrium conditions may not be reached instantaneously and Zevi et al. (2005) reported that Eq. [25] did not provide a good prediction of their observed water film thickness of between 5 and 25 μm.

When steady-state and unit hydraulic gradient water flow occurs in a nonspherical capillary, the configuration of the water along the angular capillary is determined using Eq. [24] and [25]. The water velocity distribution was obtained by numerically solving the Navier–Stokes equations (Eq. [18]) for steady-state laminar flow conditions using the COMSOL software package. A no-slip boundary condition was imposed at all SWIs, and Eq. [19] was used as the boundary condition at the AWIs. For the case of a fully saturated capillary, normal pressure differences between the inlet and outlet of the cell can be selected to achieve various average water velocities.

Figure 4 presents a plot of the velocity distribution in the saturated (Fig. 4a) and unsaturated (Fig. 4b) pore space when the average pore water velocity is 0.02 m d^{-1}. Under saturated

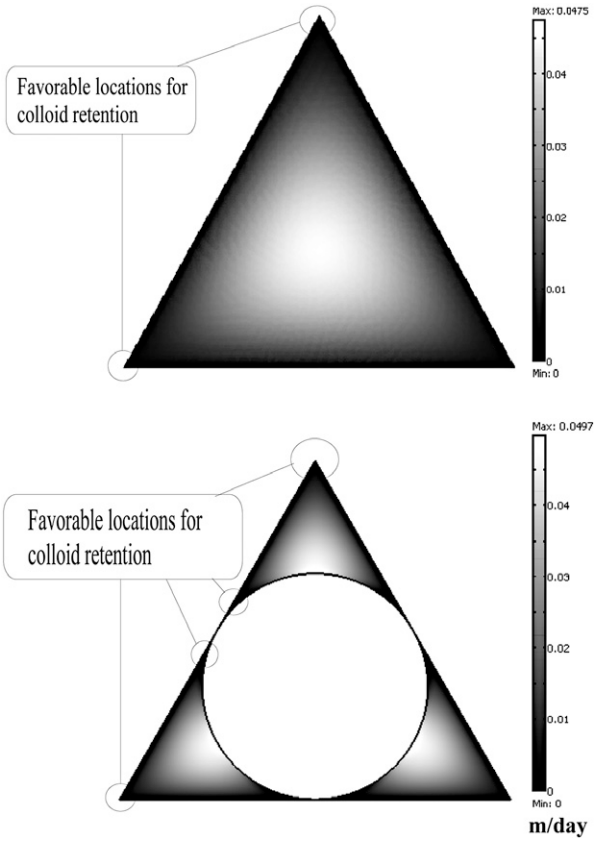

FIG. 4. The velocity distribution in (a) saturated and (b) unsaturated triangular capillary tubes when the average pore water velocity was 0.02 m d^{-1}.

conditions, zones of relative flow stagnation occur in the smallest regions of the pore space where SWIs intersect (grain–grain contact points). In addition to these locations, unsaturated flow conditions also produce low-velocity regions near the solid–water–air triple point and on thin water films adjacent to solid surfaces. It should be mentioned that porous media may be represented as a bundle of tortuous capillaries of various geometries (e.g., Tuller et al., 1999). When a given hydraulic gradient is applied to a bundle of capillaries, lower flow rates occur in smaller capillaries and in the smaller regions (corners) of unsaturated pore spaces (Fig. 4b). Figure 3 suggests that variations in the pore-scale fluid distribution will also influence colloid retention. This finding is supported by recent simulation results from a stochastic stream tube model for colloid transport and deposition (Bradford and Toride, 2007).

The rate of mass transfer to the SWIs and AWIs can be determined at the pore scale by solving the advection–diffusion equation (Eq. [21]) and assuming a perfect sink for the colloids at these interfaces. To date, no correlation equations for the colloid mass transfer to the SWI or AWI have been developed for unsaturated systems; however, Torkzaban et al. (2006a) suggested that the limited virus movement under unsaturated conditions was due to increased virus mass transfer to the SWI as a result of the reduced diffusive length in unsaturated compared with saturated systems.

In contrast to the collector scale, only a fraction of the pore space may be physically accessible to colloids as a result of their size in unsaturated porous media. This size exclusion affects the mobility of colloids by constraining them to more conductive flow domains and larger pore spaces that are hydraulically accessible. Hence, colloids may be transported faster than a conservative solute tracer (Reimus, 1995; Cumbie and McKay, 1999; Harter et al., 2000; Bradford et al., 2003; Ryan and Elimelech, 1996; Ginn, 2002). The colloid-accessible fraction of the pore space will decrease with increasing colloid size, decreasing collector size, and decreasing water saturation (Bradford et al., 2006a). For example, pore-size distribution information for average characteristics of sand, silt, and clay soils indicates that under saturated conditions, 10.5, 36.1, and 83.3% of the pore space, respectively, will be smaller than 1-μm colloids.

The forces and torques that act on colloids that are attached to the SWI and the AWI can also be determined at the pore scale. As mentioned above, the flow field is strongly influenced by the pore geometry, and low values of F_D occur at the junction of multiple SWIs or AWIs (Fig. 4). In analogy to surface roughness (Hubbe, 1984; Das et al., 1994; Burdick et al., 2005; Hoek and Agarwal, 2006), the lever arms that act on the adhesive and applied torques is also likely to depend on the pore space geometry near contact points. Steenhuis et al. (2006) reported that the vertical component of the capillary force acts to pin colloids at the solid–water–air triple point. All of these factors indicate that greater retention of colloids is expected in the smallest regions of the pore space formed near multiple interfaces than compared with smooth collector surfaces. Furthermore, the unsaturated water conductivity also rapidly decreases with decreasing water saturation (van Genuchten et al., 1991). Hence, for a given hydraulic gradient, the hydrodynamic forces that act on attached colloids in unsaturated systems are expected to be much lower than under saturated systems.

The above discussion indicates that colloids that are retained near multiple interfaces (SWI–SWI, SWI–AWI, AWI–AWI, SWI–colloid interface, AWI–colloid interface, and colloid–colloid interface) experience different forces and torques than those on a single interface. Hence, colloid retention at the pore scale may occur by processes other than attachment on a single interface. Various terms for colloid retention at the pore scale have been applied in the literature and there is not yet a consensus on this terminology. Figure 5 presents a schematic of the various pore-scale colloid retention processes that have been proposed in the literature. In saturated systems, colloid attachment may occur on the SWI (Location 1). Retention of colloids at two bounding SWIs (Location 3) has been referred to as *wedging* (Herzig et al., 1970; Johnson et al., 2007b) or *straining* (Hill, 1957; Cushing and Lawler, 1998; Bradford et al., 2006a). When multiple colloids collide and are retained in a pore constriction (Location 4), this process has been referred to as *bridging* (Ramachandran and Fogler, 1999) or *straining* (Herzig et al., 1970; Bradford et al., 2002). When all of the pore spaces in a porous medium are smaller than the colloid diameter, then complete retention of these colloids occurs via mechanical filtration (McDowell-Boyer et al., 1986). In addition to these saturated retention processes, other related colloid-retention mechanisms may occur in unsaturated systems. Colloid attachment can occur at the AWI (Location 2). *Film straining* refers to retention of colloids in thin water films that are smaller than the colloid diameter (Location 6) (Wan and Tokunaga, 1997), and colloids may also be retained at the solid–water–air triple point (Location 5) (Crist et al., 2004, 2005; Chen and Flury, 2005) in much that same way as wedging at grain-to-grain contact points. It should be noted that colloids that are retained at the triple point may experience DLVO and hydrophobic forces that are associated with the SWI and AWI, as well as capillary forces if they penetrate the AWI (Chen and Flury, 2005). In this work, we refer to retention of colloids on a

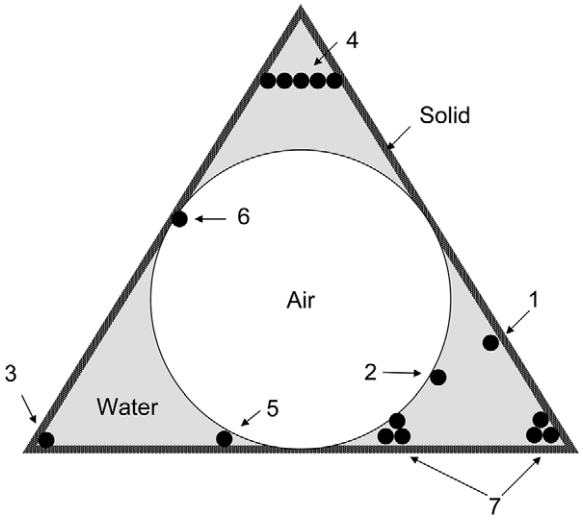

FIG. 5. A schematic of the various pore-scale colloid retention processes. Colloid retention at Locations 1 and 2 occurs via attachment to the solid–water and air–water interfaces, respectively. Colloid retention at Locations 3, 4, 5, and 7 occurs via various straining mechanisms, namely: 3, wedging; 4, bridging; 5, retention at the solid–water–air triple point; and 6, film straining. Locations 3, 4, 5, and 7 correspond to the more general definition of straining as colloid retention in the smallest regions of the pore space.

single interface (SWI or AWI) as *attachment*. Retention of colloids at multiple interfaces (wedging, bridging, film straining, and retention at the triple point) share many similarities (low-velocity regions), and can all be encompassed by the more general definition of straining as colloid retention in the smallest regions of the pore space (Locations 7) (McDowell-Boyer et al., 1986; Bradford et al., 2002, 2003, 2004, 2005, 2006a,b; Tufenkji et al., 2004; Foppen et al., 2005; Xu et al., 2006; Yoon et al., 2006).

Straining processes have only recently begun to receive research attention, and there are still many questions that have not yet been resolved. As the water saturation decreases in water-wet porous media, water is held by capillary forces in successively smaller regions of the pore space. Hence, a greater fraction of the mobile colloids will be transported through regions of the pore space where straining processes may occur. Wedging, bridging, and retention at the triple point are therefore all expected to increase with decreasing water saturation, but this dependency has not been quantified and it may not be possible to mechanistically separate the influence of all of these individual straining processes. The water film thickness will also decrease with decreasing water saturation. If water films envelop colloids, then film straining will occur. Temporal changes in water saturation during drainage and infiltration processes have also been demonstrated to have important roles in colloid retention and release (Saiers et al., 2003; Saiers and Lenhart, 2003; Torkzaban et al., 2006a; Zhuang et al., 2007) due to changes in the air–water interfacial area, scavenging of colloids by moving solid–water–air triple points, and by changes in the water-filled portion of the pore space. It should be mentioned that colloids that have been retained by film straining or a moving solid–water–air triple point may be more strongly retained at the AWI because of the presence of capillary forces, and temporal changes in the water saturation may therefore mobilize these colloids.

Straining processes have traditionally been assumed to be purely physical phenomena (Herzig et al., 1970; McDowell-Boyer et al., 1986) and therefore only determined by geometry considerations. Recent experimental evidence, however, has indicated a strong coupling of straining processes on solution chemistry and hydrodynamics (Bradford et al., 2006a, 2007; Torkzaban et al., 2008). Insight into the roles of solution chemistry and hydrodynamics on straining processes can be obtained from Fig. 3. This figure indicates that hydrodynamic and adhesive forces will have a big impact on the fraction of the collector surface where retention occurs, and that colloids that collide with a collector may roll along the surface until they come to a region that is chemically and hydrodynamically favorable for deposition. Figure 4 indicates that these favorable retention locations occur where multiple interfaces intersect (zones of relative flow stagnation). Increasing the adhesive force or decreasing the pore-water velocity will direct and retain a larger number of colloids in a given porous medium (Bradford et al., 2007). It is interesting to note that a reduction of the adhesive force will only liberate a fraction of the colloids retained in a given straining location, and that this fraction will depend on the relative size of the colloid and median grain diameter (Bradford et al., 2007).

Many research issues with regard to straining processes in saturated and unsaturated porous media still need to be addressed and quantified. For example, bridging is expected to be a function of solution chemistry, hydrodynamics, and colloid concentration, but this dependency is likely to be different than colloid retention at the triple point and wedging locations due to differences in the hydrodynamics and pore space configurations. It has been reported that bridging increases with increasing hydrodynamic forces and colloid concentration (Ramachandran and Fogler, 1999), whereas Fig. 3 suggests that retention at locations of grain–grain contacts will decrease with increasing hydrodynamic forces and colloid concentration (S_f fills more rapidly at a higher concentration). It is also possible that colloid aggregation may play a role in colloid retention at all of these straining locations (Bradford et al., 2006b), and this process is expected to be a function of hydrodynamics and the chemistry of the colloids and the solution. Additional research is also needed to quantify and to model the influence of temporal changes in solution chemistry and hydrodynamics on colloid retention and release.

Time- and concentration-dependent retention of the colloids in straining locations is to be expected due to filling of these locations (Foppen et al., 2005; Bradford and Bettahar, 2006). If the colloid size is known, then the number of colloids that is required to fill a given volume of the porous medium can be calculated (Foppen et al., 2005). The rate of filling of these sites is theoretically dependent on the concentration of the colloids in suspension (e.g., higher colloid concentrations fill straining sites more rapidly than low concentrations). Large numbers of colloids will be required to fill even small straining fractions of the pore space. As accessible straining sites become filled, water and colloids may be diverted from these regions and less colloid retention will occur with increasing time. Alternatively, straining processes may also produce clogging of pores that will lead to permeability reductions in the porous media. Reviews of colloid-induced clogging of porous media have recently been given by Baveye et al. (1998) and Mays and Hunt (2005).

Conclusions

Our ability to accurately simulate colloid transport and retention in aquifers, and especially in the vadose zone, is currently limited by our lack of basic understanding of the governing processes that control colloid retention at the pore scale. This review discussed our current understanding of physical and chemical mechanisms, factors, and models of colloid transport and retention at the interface, collector, and pore scales. We have identified gaps in knowledge, and provided recommendations and illustrative examples of how to tackle these challenges at the pore scale.

The interface scale is well suited for studying the interaction energy and hydrodynamic forces and torques of colloids near solid–water, air–water, and colloid–colloid interfaces. The DLVO theory provides a useful approach to predict these interactions for various system conditions (zeta potentials of colloids and interfaces, solution ionic strengthen, and colloid size). The DLVO theory, however, does not account for non-DLVO forces such as hydrophobic and capillary forces that may also play a significant role in colloid attachment to the AWI. At present, non-DLVO interactions are incompletely understood and quantitative theory has not been developed or is not generally accepted. Surface roughness is reported to have a significant influence on both adhesive and applied hydrodynamic torques that act on colloids near solid interfaces.

At the single-collector scale, the aqueous flow field can be solved and the rate of mass transfer to a collector surface (solid grain or air bubble) can be calculated. Lower velocities occur adjacent to a spherical solid grain collector compared with an air bubble of similar size due to different boundary conditions at the interface (no slip compared with Eq. [19]). A balance of adhesive and applied hydrodynamic torques (rolling) that act on colloids that collide with a solid collector indicates that only a fraction of the collector surface may contribute to attachment due to variations in the flow field around the collector. The fraction of the collector surface that contributes to attachment will depend on both physical (water velocity and collector shape and size) and chemical (pH, ionic strength, zeta potentials of colloids and collectors, and surface charge heterogeneity) conditions. In contrast to the solid collector, colloids that collide with an air bubble collector will probably slide along this surface due to the presence of a relatively uniform water flow field adjacent to this interface and a low coefficient of sliding friction.

Similar to the collector scale, the flow field can be solved and the rate of mass transfer to an interface can be determined at the pore scale. Differences in flow, mass transfer, and colloid retention processes occur, however, due to the presence of multiple solid–water and air–water interfaces and contact points (grain–grain contacts and the solid–water–air triple point). Specifically, low-velocity regions occur near these contact points. These differences in the flow field and smaller diffusion path lengths that occur in unsaturated systems will influence the colloid mass flux to a particular interface. At present, no mass transfer correlations have been developed for truly pore-scale geometries or for unsaturated systems. Colloid retention mechanisms will also be influenced by the pore space geometry. At the pore scale, a variety of straining processes may occur in saturated (wedging and bridging) and unsaturated (wedging, bridging, film straining, and retention at the triple point) systems, as well as colloid size exclusion. Current knowledge of straining processes is still incomplete but recent research indicates a strong coupling of hydrodynamics, solution chemistry, and colloid concentration on these processes, as well as a dependency on the colloid and grain sizes and the water content.

Acknowledgments

This research was supported by the 206 Manure and Byproduct Utilization Project of the USDA-ARS and by a grant from NRI (NRI no. 2006-02541). Mention of trade names and company names in this manuscript does not imply any endorsement or preferential treatment by the USDA.

References

Abbaszadegan, M., M.W. LeChevallier, and C.P. Gerba. 2003. Occurrence of viruses in US groundwaters. J. Am. Water Works Assoc. 95:107–120.

Abdel-Fattah, A.I., and M.S. El-Genk. 1998. On colloidal particle sorption onto a stagnant air–water interface. Adv. Colloid Interface Sci. 78:237–266.

Abudalo, R.A., Y.G. Bogatsu, J.N. Ryan, R.W. Harvey, D.W. Metge, and M. Elimelech. 2005. The effect of ferric oxyhydroxide grain coatings on the transport of bacteriophage PRD1 and *Cryptosporidium parvum* oocysts in saturated porous media. Environ. Sci. Technol. 39:6412–6419.

Adamczyk, Z., B. Siwek, M. Zembala, and P. Belouschek. 1994. Kinetics of localized adsorption of colloid particles. Adv. Colloid Interface Sci. 48:151–280.

Ahmadi, M., and Q. Chen. 1998. Dispersion and deposition of particles in a turbulent pipe flow with sudden expansion. J. Aerosol Sci. 29:1097–1116.

Albinger, O., B.K. Biesemeyer, R.G. Arnold, and B.E. Logan. 1994. Effect of bacterial heterogeneity on adhesion to uniform collectors by monoclonal populations. FEMS Microbiol. Lett. 124:321–326.

Auset, M., and A.A. Keller. 2004. Pore-scale processes that control dispersion of colloids in saturated porous media. Water Resour. Res. 40:W03503, doi:10.1029/2003WR002800.

Baveye, P., P. Vandevivere, B.L. Hoyle, P.C. Deleo, and D. Sanchez de Lozada. 1998. Environmental impact and mechanisms of the biological clogging of saturated soils and aquifer materials. Crit. Rev. Environ. Sci. Technol. 28:123–191.

Baygents, J.C., J.R. Glynn, Jr., O. Albinger, B.K. Biesemeyer, K.L. Ogden, and R.G. Arnold. 1998. Variation of surface charge density in monoclonal bacterial populations: Implications for transport through porous media. Environ. Sci. Technol. 32:1596–1603.

Bergendahl, J., and D. Grasso. 1998. Colloid generation during batch leaching tests: Mechanics of disaggregation. Colloids Surf. A 135:193–205.

Bergendahl, J., and D. Grasso. 1999. Prediction of colloid detachment in a model porous media: Thermodynamics. AIChE J. 45:475–484.

Bergendahl, J., and D. Grasso. 2000. Prediction of colloid detachment in a model porous media: Hydrodynamics. Chem. Eng. Sci. 55:1523–1532.

Bird, R.B., W.E. Stewart, and E.N. Lightfoot. 2002. Transport phenomena. 2nd ed. John Wiley & Sons, New York.

Bolster, C.H., A.L. Mills, G.M. Hornberger, and J.S. Herman. 1999. Spatial distribution of deposited bacteria following miscible displacement experiments in intact cores. Water Resour. Res. 35:1797–1807.

Bolster, C.H., A.L. Mills, G. Hornberger, and J. Herman. 2000. Effect of intrapopulation variability on the long-distance transport of bacteria. Ground Water 38:370–375.

Bradford, S.A., and M. Bettahar. 2005. Straining, attachment, and detachment of *Cryptosporidium* oocysts in saturated porous media. J. Environ. Qual. 34:469–478.

Bradford, S.A., and M. Bettahar. 2006. Concentration dependent colloid transport in saturated porous media. J. Contam. Hydrol. 82:99–117.

Bradford, S.A., M. Bettahar, J. Šimůnek, and M.Th. van Genuchten. 2004. Straining and attachment of colloids in physically heterogeneous porous media. Vadose Zone J. 3:384–394.

Bradford, S.A., J. Šimůnek, M. Bettahar, Y.F. Tadassa, M.Th. van Genuchten, and S.R. Yates. 2005. Straining of colloids at textural interfaces. Water Resour. Res. 41:W10404, doi:10.1029/2004WR003675.

Bradford, S.A., J. Šimůnek, M. Bettahar, M.Th. van Genuchten, and S.R. Yates. 2003. Modeling colloid attachment, straining, and exclusion in saturated porous media. Environ. Sci. Technol. 37:2242–2250.

Bradford, S.A., J. Šimůnek, M. Bettahar, M.Th. van Genuchten, and S.R. Yates. 2006a. Significance of straining in colloid deposition: Evidence and implications. Water Resour. Res. 42:W12S15, doi:10.1029/2005WR004791.

Bradford, S.A., J. Šimůnek, and S.L. Walker. 2006b. Transport and straining of *E. coli* O157:H7 in saturated porous media. Water Resour. Res. 42:W12S12, doi:10.1029/2005WR004805.

Bradford, S.A., and N. Toride. 2007. A stochastic model for colloid transport and deposition. J. Environ. Qual. 36:1346–1356.

Bradford, S.A., S. Torkzaban, and S.L. Walker. 2007. Coupling of physical and chemical mechanisms of colloid straining in saturated porous media. Water Res. 41:3012–3024.

Bradford, S.A., S.R. Yates, M. Bettahar, and J. Šimůnek. 2002. Physical factors affecting the transport and fate of colloids in saturated porous media. Water Resour. Res. 38(12):1327, doi:10.1029/2002WR001340.

Breiner, J.M., M.A. Anderson, H.W.K. Tom, and R.C. Graham. 2006. Properties of surface-modified colloidal particles. Clays Clay Miner. 54:12–24.

Burdick, G.M., N.S. Berman, and S.P. Beaudoin. 2005. Hydrodynamic particle removal from surfaces. Thin Solid Films 488:116–123.

Chandrasekhar, S. 1943. Stochastic problems in physics and astronomy. Rev. Mod. Phys. 15:1–89.

Chen, G., and M. Flury. 2005. Retention of mineral colloids in unsaturated porous media as related to their surface properties. Colloids Surf. A 256:207–216.

Chen, G., M. Flury, J.B. Harsh, and P.C. Lichtner. 2005. Colloid-facilitated transport of cesium in variably saturated Hanford sediments. Environ. Sci. Technol. 39:3435–3442.

Cherrey, K.D., M. Flury, and J.B. Harsh. 2003. Nitrate and colloid transport through coarse Hanford sediments under steady state, variably saturated flow. Water Resour. Res. 39(6):1165, doi:10.1029/2002WR001944.

Choi, H., and M.Y. Corapcioglu. 1997. Transport of a non-volatile contaminant in unsaturated porous media in the presence of colloids. J. Contam. Hydrol. 25:299–324.
Chu, Y., Y. Jin, and M.V. Yates. 2001. Mechanisms of virus removal during transport in unsaturated porous media. Water Resour. Res. 37:253–263.
Cooper, K., A. Gupta, and S. Beaudoin. 2000a. Substrate morphology and particle adhesion in reacting systems. J. Colloid Interface Sci. 228:213–219.
Cooper, K., A. Gupta, and S. Beaudoin. 2001. Simulation of the adhesion of particles to surfaces. J. Colloid Interface Sci. 234:284–292.
Cooper, K., N. Ohler, A. Gupta, and S. Beaudoin. 2000b. Analysis of contact interactions between a rough deformable colloid and a smooth substrate. J. Colloid Interface Sci. 222:63–74.
Crist, J.T., J.F. McCarthy, Y. Zevi, P. Baveye, J.A. Throop, and T.S. Steenhuis. 2004. Pore-scale visualization of colloid transport and retention in partly saturated porous media. Vadose Zone J. 3:444–450.
Crist, J.T., Y. Zevi, J.F. McCarthy, J.A. Throop, and T.S. Steenhuis. 2005. Transport and retention mechanisms of colloids in partially saturated porous media. Vadose Zone J. 4:184–195.
Cumbie, D.H., and L.D. McKay. 1999. Influence of diameter on particle transport in a fractured shale saprolite. J. Contam. Hydrol. 37:139–157.
Cushing, R.S., and D.F. Lawler. 1998. Depth filtration: Fundamental investigation through three-dimensional trajectory analysis. Environ. Sci. Technol. 32:3793–3801.
Das, S.K., R.S. Schechter, and M.M. Sharma. 1994. The role of surface roughness and contact deformation on the hydrodynamic detachment of particles from surfaces. J. Colloid Interface Sci. 164:63–77.
Davis, J.A. 1982. Adsorption of dissolved natural organic matter at the oxide/water interface. Geochim. Cosmochim. Acta 46:2381–2393.
DeFlaun, M.F., C.J. Murray, M. Holben, T. Scheibe, A. Mills, T. Ginn, T. Griffin, E. Majer, and J.L. Wilson. 1997. Preliminary observations on bacterial transport in a coastal plain aquifer. FEMS Microbiol. Rev. 20:473–487.
de Jonge, L.W., C. Kjaergaard, and P. Moldrup. 2004. Colloids and colloid-facilitated transport of contaminants in soils: An introduction. Vadose Zone J. 3:321–325.
DeNovio, N.M., J.E. Saiers, and J.N. Ryan. 2004. Colloid movement in unsaturated porous media: Recent advances and future directions. Vadose Zone J. 3:338–351.
Derjaguin, B.V., and L.D. Landau. 1941. Theory of the stability of strongly charged lyophobic sols and of the adhesion of strongly charged particles in solutions of electrolytes. Acta Physicochim. URSS 14:733–762.
Dong, H., T.C. Onstott, C.-H. Ko, A.D. Hollingsworth, D.G. Brown, and B.J. Mailloux. 2002. Theoretical prediction of collision efficiency between adhesion-deficient bacteria and sediment grain surface. Colloids Surf. B 24:229–245.
Ducker, W.A., Z. Xu, and J.N. Israelachvili. 1994. Measurements of hydrophobic and DLVO forces in bubble-surface interactions in aqueous solutions. Langmuir 10:3279–3289.
Elimelech, M., J. Gregory, X. Jia, and R.A. Williams. 1998. Particle deposition and aggregation measurement, modeling, and simulation. Butterworth-Heinemann, Woburn, MA.
Elimelech, M., M. Nagai, C.-H. Ko, and J.N. Ryan. 2000. Relative insignificance of mineral grain zeta potential to colloid transport in geochemically heterogeneous porous media. Environ. Sci. Technol. 34:2143–2148.
Elimelech, M., and C.R. O'Melia. 1990. Kinetics of deposition of colloidal particles in porous media. Environ. Sci. Technol. 24:1528–1536.
Foppen, J.W.A., A. Mporokoso, and J.F. Schijven. 2005. Determining straining of *Escherichia coli* from breakthrough curves. J. Contam. Hydrol. 76:191–210.
Franchi, A., and C.R. O'Melia. 2003. Effects of natural organic matter and solution chemistry on the deposition and reentrainment of colloids in porous media. Environ. Sci. Technol. 37:1122–1129.
Gargiulo, G., S.A. Bradford, J. Šimůnek, H. Vereecken, and E. Klumpp. 2006. Transport and deposition of metabolically active and stationary phase *Deinococcus radiodurans* in unsaturated porous media. Environ. Sci. Technol. 41:1265–1271.
Gerba, C.P., J.B. Rose, and C.N. Haas. 1996. Sensitive populations: Who is at the greatest risk? Int. J. Food Microbiol. 30:113–123.
Gerba, C.P., and J.E. Smith, Jr. 2005. Sources of pathogenic microorganisms and their fate during land application of wastes. J. Environ. Qual. 34:42–48.
Ginn, T.R. 2002. A travel time approach to exclusion on transport in porous media. Water Resour. Res. 38(4):1041, doi:10.1029/2001WR000865.
Ginn, T.R., B.D. Wood, K.E. Nelson, T.D. Schiebe, E.M. Murphy, and T.P. Clement. 2002. Processes in microbial transport in the natural subsurface. Adv. Water Res. 25:1017–1042.
Goldman, A.J., R.G. Cox, and H. Brenner. 1967. Slow viscous motion of a sphere parallel to a plane wall: I. Motion through a quiescent fluid. Chem. Eng. Sci. 22:637–651.
Grasso, D., K. Subramaniam, M. Butkus, K. Strevett, and J. Bergendahl. 2002. A review of non-DLVO interactions in environmental colloidal systems. Rev. Environ. Sci. Biotechnol. 1:17–38.
Gregory, J. 1981. Approximate expression for retarded van der Waals interaction. J. Colloid Interface Sci. 83:138–145.
Grolimund, D., M. Borkovec, K. Barmettler, and H. Sticher. 1996. Colloid-facilitated transport of strongly sorbing contaminants in natural porous media: A laboratory column study. Environ. Sci. Technol. 30:3118–3123.
Gschwend, P.M., and M.D.J. Reynolds. 1987. Monodisperse ferrous phosphate colloids in an anoxic groundwater plume. J. Contam. Hydrol. 1:309–327.
Gupta, D., and M.H. Peters. 1985. A Brownian dynamics simulation of aerosol deposition onto spherical collectors. J. Colloid Interface Sci. 104:375–389.
Hahn, M.W., D. Abadzic, and C.R. O'Melia. 2004. Aquasols: On the role of secondary minima. Environ. Sci. Technol. 38:5915–5924.
Hahn, M.W., and C.R. O'Melia. 2004. Deposition and reentrainment of Brownian particles in porous media under unfavorable chemical conditions: Some concepts and applications. Environ. Sci. Technol. 38:210–220.
Happel, J. 1958. Viscous flow in multiparticle systems: Slow motion of fluids relative to beds of spherical particles. AIChE J. 4:197–201.
Harter, T., S. Wagner, and E.R. Atwill. 2000. Colloid transport and filtration of *Cryptosporidium parvum* in sandy soils and aquifer sediments. Environ. Sci. Technol. 34:62–70.
Harvey, R.W., and H. Harms. 2002. Transport of microorganisms in the terrestrial subsurface: In situ and laboratory methods. p. 753–776. *In* C.J. Hurst et al. (ed.) Manual of environmental microbiology. 2nd ed. ASM Press, Herndon, VA.
Herzig, J.P., D.M. Leclerc, and P. LeGoff. 1970. Flow of suspension through porous media: Application to deep filtration. Ind. Eng. Chem. 62:129–157.
Hill, W.A. 1957. An analysis of sand filtration. J. Sanitary Eng. Div. Am. Soc. Civ. Eng. 83(SA3):1276-1–1276-9.
Hoek, E.M.V., and G.K. Agarwal. 2006. Extended DLVO interactions between spherical particles and rough surfaces. J. Colloid Interface Sci. 298:50–58.
Hogg, R., T.W. Healy, and D.W. Fuerstenau. 1966. Mutual coagulation of colloidal dispersions. Trans. Faraday Soc. 62:1638–1651.
Hubbe, M.A. 1984. Theory of detachment of colloidal particles from flat surfaces exposed to flow. Colloids Surf. 12:151–178.
Israelachvili, J.N. 1992. Intermolecular and surface forces. 2nd ed. Academic Press, London.
Iwamatsu, M., and K. Horii. 1996. Capillary condensation and adhesion of two wetter surfaces. J. Colloid Interface Sci. 182:400–406.
Jin, Y., and M. Flury. 2002. Fate and transport of viruses in porous media. Adv. Agron. 77:39–102.
Johnson, D.J., N.J. Miles, and N. Hilal. 2006. Quantification of particle–bubble interactions using atomic force microscopy: A review. Adv. Colloid Interface Sci. 127:67–81.
Johnson, K.L. 1985. Contact mechanics. Cambridge Univ. Press, Cambridge, UK.
Johnson, K.L., K. Kendall, and A.D. Roberts. 1971. Surface energy and the contact of elastic solids. Proc. R. Soc. London Ser. A 11:301–313.
Johnson, P.R., and M. Elimelech. 1995. Dynamics of colloid deposition in porous media: Blocking based on random sequential adsorption. Langmuir 11:801–812.
Johnson, W.P., and X. Li. 2005. Comment on "Breakdown of colloid filtration theory: Role of secondary energy minimum and surface charge heterogeneities." Langmuir 21:10895.
Johnson, W.P., X. Li, and S. Assemi. 2007a. Deposition and re-entrainment dynamics of microbes and non-biological colloids during non-perturbed transport in porous media in the presence of an energy barrier to deposition. Adv. Water Resour. 30:1432–1454.
Johnson, W.P., X. Li, and G. Yal. 2007b. Colloid retention in porous media: Mechanistic confirmation of wedging and retention in zones of flow stagnation. Environ. Sci. Technol. 41:1279–1287.

Kelsall, G.H., S. Tang, S. Yurdakul, and A.L. Smith. 1996. Electrophoretic behaviour of bubbles in aqueous electrolytes. J. Chem. Soc. Faraday Trans. 92:3887–3893.

Khilar, K.C., and H.S. Fogler. 1998. Migration of fines in porous media. Kluwer Acad. Publ., Dordrecht, the Netherlands.

Kim, J.I. 1991. Actinide colloid generation in groundwater. Radiochim. Acta 52/53:71–81.

Kim, M.M., and A.L. Zydney. 2004. Effect of electrostatic, hydrodynamic, and Brownian forces on particle trajectories and sieving in normal flow filtration. J. Colloid Interface Sci. 269:425–431.

Kim, S.B., M.Y. Corapcioglu, and D.J. Kim. 2003. Effect of dissolved organic matter and bacteria on contaminant transport in riverbank filtration. J. Contam. Hydrol. 66:1–23.

Kretzschmar, R., K. Barmettler, D. Grolimun, Y.D. Yan, M. Borkovec, and H. Sticher. 1997. Experimental determination of colloid deposition rates and collision efficiencies in natural porous media. Water Resour. Res. 33:1129–1137.

Kuznar, Z.A., and M. Elimelech. 2007. Direct microscopic observation of particle deposition in porous media: Role of the secondary energy minimum. Colloids Surf. A 294:156–162.

Lance, J.C., and C.P. Gerba. 1984. Virus movement in soil during saturated and unsaturated flow. Appl. Environ. Microbiol. 47:335–341.

Lazouskaya, V., Y. Jin, and D. Or. 2006. Interfacial interactions and colloid retention under steady flows in a capillary channel. J. Colloid Interface Sci. 303:171–184.

Lenormand, R., C. Zarcone, and A. Sarr. 1983. Mechanisms of the displacement of one fluid by another in a network of capillary ducts. J. Fluid Mech. 135:337–353.

Li, X., and W.P. Johnson. 2005. Non-monotonic variations in removal rate coefficients of microspheres in porous media under unfavorable deposition conditions. Environ. Sci. Technol. 39:1658–1665.

Li, X., C.-L. Lin, J.D. Miller, and W.P. Johnson. 2006. Pore-scale observation of microsphere deposition at grain-to-grain contacts over assemblage-scale porous media domains using x-ray microtomography. Environ. Sci. Technol. 40:3762–3768.

Li, X., T.D. Scheibe, and W.P. Johnson. 2004. Apparent decreases in colloid deposition rate coefficient with distance of transport under unfavorable deposition conditions: A general phenomenon. Environ. Sci. Technol. 38:5616–5625.

Li, X., P. Zhang, C.L. Lin, and W.P. Johnson. 2005. Role of hydrodynamic drag on microsphere deposition and re-entrainment in porous media under unfavorable conditions. Environ. Sci. Technol. 39:4012–4020.

Li, Y., and N.C. Wardlaw. 1986. Mechanisms of nonwetting phase trapping during imbibition at slow rates. J. Colloid Interface Sci. 109:473–486.

Liu, D., P.R. Johnson, and M. Elimelech. 1995. Colloid deposition dynamics in flow-through porous media: Role of electrolyte concentration. Environ. Sci. Technol. 29:2963–2973.

Logan, B.E., D.G. Jewett, R.G. Arnold, E.J. Bouwer, and C.R. O'Melia. 1995. Clarification of clean-bed filtration models. J. Environ. Eng. 121:869–873.

Loge, F.J., D.E. Thompson, and R.C. Douglas. 2002. PCR detection of specific pathogens in water: A risk-based analysis. Environ. Sci. Technol. 36:2754–2759.

Mason, G., and N.R. Morrow. 1984. Meniscus curvatures in capillaries of uniform cross-section. J. Chem. Soc. Faraday Trans. 1 80:2375–2393.

Mason, G., and N.R. Morrow. 1991. Capillary behavior of a perfectly wetting liquid in irregular triangular tubes. J. Colloid Interface Sci. 141:262–274.

Mays, D.C., and J.R. Hunt. 2005. Hydrodynamic aspects of particle clogging in porous media. Environ. Sci. Technol. 39:577–584.

McCarthy, J.F., and J.M. Zachara. 1989. Subsurface transport of contaminants. Environ. Sci. Technol. 23:496–502.

McDowell-Boyer, L.M., J.R. Hunt, and N. Sitar. 1986. Particle transport through porous media. Water Resour. Res. 22:1901–1921.

Mishra, S., J. Jeevan, C.K. Ramesh, and L. Banwari. 2001. In situ bioremediation potential of an oily sludge-degrading bacterial consortium. Curr. Microbiol. 43:328–335.

Nyhan, J.W., B.J. Brennon, W.V. Abeele, M.L. Wheeler, W.D. Purtymun, G. Trujillo, W.J. Herrera, and J.W. Booth. 1985. Distribution of plutonium and americium beneath a 33-yr-old liquid waste disposal site. J. Environ. Qual. 14:501–509.

Ochiai, N., E.L. Kraft, and J.S. Selker. 2006. Methods for colloid transport visualization in pore networks. Water Resour. Res. 42:W12S06, doi:10.1029/2006WR004961.

O'Neill, M.N. 1968. A sphere in contact with a plane wall in a slow linear shear flow. Chem. Eng. Sci. 23:1293–1298.

Ouyang, Y., D. Shinde, R.S. Mansell, and W. Harris. 1996. Colloid-enhanced transport of chemicals in subsurface environments: A review. Crit. Rev. Environ. Sci. Technol. 26:189–204.

Payatakes, A.C., R. Rajagopalan, and C. Tien. 1974. On the use of Happel's model for filtration studies. J. Colloid Interface Sci. 49:321.

Rabinovich, Ya.I., and R.-H. Yoon. 1994. Use of atomic force microscope for the measurements of hydrophobic forces between silanated silica plate and glass sphere. Langmuir 10:1903–1909.

Rajagopalan, R., and C. Tien. 1976. Trajectory analysis of deep-bed filtration with the sphere-in-cell porous-media model. AIChE J. 22:523–533.

Ramachandran, V., and H.S. Fogler. 1999. Plugging by hydrodynamic bridging during flow of stable colloidal particles within cylindrical pores. J. Fluid Mech. 385:129–156.

Ray, C., T.W. Soong, Y.Q. Lian, and G.S. Roadcap. 2002. Effect of flood-induced chemical load on filtrate quality at bank filtration sites. J. Hydrol. 266:235–258.

Redman, J.A., S.B. Grant, T.M. Olson, and M.K. Estes. 2001. Pathogen filtration, heterogeneity, and the potable reuse of wastewater. Environ. Sci. Technol. 35:1798–1805.

Redman, J.A., S.L. Walker, and M. Elimelech. 2004. Bacterial adhesion and transport in porous media: Role of the secondary energy minimum. Environ. Sci. Technol. 38:1777–1785.

Reimus, P.W. 1995. The use of synthetic colloids in tracer transport experiments in saturated rock fractures. LA-13004-T. Los Alamos National Lab., Los Alamos, NM.

Rockhold, M.L., R.R. Yarwood, and J.S. Selker. 2004. Coupled microbial and transport processes in soils. Vadose Zone J. 3:368–383.

Ryan, J.N., and M. Elimelech. 1996. Colloid mobilization and transport in groundwater. Colloids Surf. A 107:1–56.

Ryan, J.N., and P.M. Gschwend. 1990. Colloid mobilization in two Atlantic Coastal Plain aquifers: Field studies. Water Resour. Res. 26:307–322.

Saffman, P.G. 1965. The lift on a small sphere in a slow shear flow. J. Fluid Mech. 22:385–400.

Saiers, J.E., G.M. Hornberger, D.B. Gower, and J.S. Herman. 2003. The role of moving air–water interfaces in colloid mobilization within the vadose zone. Geophys. Res. Lett. 30(21):2083, doi:10.1029/2003GL018418.

Saiers, J.E., and J.J. Lenhart. 2003. Colloid mobilization and transport within unsaturated porous media under transient-flow conditions. Water Resour. Res. 39(1):1019, doi:10.1029/2002WR001370.

Saiers, J.E., and J.N. Ryan. 2005. Colloid deposition on non-ideal porous media: The influences of collector shape and roughness on the single-collector efficiency. Geophys. Res. Lett. 32:L21406, doi:10.1029/2005GL024343.

Schafer, A., H. Harms, and A.J.B. Zehnder. 1998a. Bacterial accumulation at the air–water interface. Environ. Sci. Technol. 32:3704–3712.

Schafer, A., P. Ustohal, H. Harms, F. Stauffer, T. Dracos, and A.J.B. Zehnder. 1998b. Transport of bacteria in unsaturated porous media. J. Contam. Hydrol. 33:149–169.

Schijven, J.K., and S.M. Hassanizadeh. 2000. Removal of viruses by soil passage: Overview of modeling, processes, and parameters. Crit. Rev. Environ. Sci. Technol. 30:49–127.

Sen, T.K., and K.C. Khilar. 2006. Review on subsurface colloids and colloid-associated contaminant transport in saturated porous media. Adv. Colloid Interface Sci. 119:71–96.

Simoni, S.F., H. Harms, T.N.P. Bosma, and A.J.B. Zehnder. 1998. Population heterogeneity affects transport of bacteria through sand columns at low flow rates. Environ. Sci. Technol. 32:2100–2105.

Šimůnek, J., C. He, L. Pang, and S.A. Bradford. 2006. Colloid-facilitated transport in variably saturated porous media: Numerical model and experimental verification. Vadose Zone J. 5:1035–1047.

Sirivithayapakorn, S., and A. Keller. 2003a. Transport of colloids in saturated porous media: A pore-scale observation of the size exclusion effect and colloid acceleration. Water Resour. Res. 39(4):1109, doi:10.1029/2002WR001583.

Sirivithayapakorn, S., and A. Keller. 2003b. Transport of colloids in unsaturated porous media: A pore-scale observation of processes during the dissolution of air–water interface. Water Resour. Res. 39(12):1346, doi:10.1029/2003WR002487.

Soltani, M., and G. Ahmadi. 1994. On particle adhesion and removal mechanics in turbulent flows. J. Adhes. Sci. Technol. 8:763–785.

Song, L., and M. Elimelech. 1993. Dynamics of colloid deposition in porous media: Modeling the role of retained particles. Colloids Surf. A 73:49–63.

Song, L., and M. Elimelech. 1994. Transient deposition of colloidal particles in heterogeneous porous media. J. Colloid Interface Sci. 167:301–313.

Steenhuis, T.S., A. Dathe, Y. Zevi, J.L. Smith, B. Gao, S.B. Shaw, et al. 2006. Biocolloid retention in partially saturated soils. Biologia 61:S229–S233.

Steenhuis, T.S., J.F. McCarthy, J.T. Crist, Y. Zevi, P.C. Baveye, J.A. Throop, R.L. Fehrman, A. Dathe, and B.K. Richards. 2005. Reply to "Comments on 'Pore-scale visualization of colloid transport and retention in partly saturated porous media.' " Vadose Zone J. 4:957–958.

Tan, Y., J.T. Cannon, P. Baveye, and M. Alexander. 1994. Transport of bacteria in an aquifer sand: Experiments and model simulations. Water Resour. Res. 30:3243–3252.

Tipping, E., and D. Cooke. 1982. The effects of adsorbed humic substances on the surface charge of goethite (α-FeOOH) in freshwaters. Geochim. Cosmochim. Acta 46:75–80.

Tong, M., and W.P. Johnson. 2007. Colloid population heterogeneity drives hyper-exponential deviation from classic filtration theory. Environ. Sci. Technol. 41:493–499.

Tong, M., X. Li, C.N. Brow, and W.P. Johnson. 2005. Detachment-influenced transport of an adhesion-deficient bacterial strain within water-reactive porous media. Environ. Sci. Technol. 39:2500–2508.

Torkzaban, S., S.A. Bradford, and S.L. Walker. 2007. Resolving the coupled effects of hydrodynamics and DLVO forces on colloid attachment in porous media. Langmuir 23:9652–9660.

Torkzaban, S., S.A. Bradford, and S.L. Walker. 2008. Colloid transport in unsaturated porous media: The role of water content and ionic strength on particle straining. J. Contam. Hydrol. 96:113–127.

Torkzaban, S., S.M. Hassanizadeh, J.F. Schijven, and A.M. de Roda Husman. 2006a. Virus transport in saturated and unsaturated sand columns. Vadose Zone J. 5:877–885.

Torkzaban, S., S.M. Hassanizadeh, J.F. Schijven, and H.H.J.L. van den Berg. 2006b. Role of air–water interfaces on retention of viruses under unsaturated conditions. Water Resour. Res. 42:W12S14, doi:10.1029/2006WR004904.

Tsai, C.J., D.Y.H. Pui, and B.Y.H. Liu. 1991. Particle detachment from disk surfaces of computer disk drives. J. Aerosol Sci. 22:737–746.

Tsao, Y.H., D.F. Evans, and H. Wennerstrom. 1993. Long-range attraction between a hydrophobic surface and a polar surface is stronger than that between two hydrophobic surfaces. Langmuir 9:779–785.

Tufenkji, N., D.R. Dixon, R. Considine, and C.J. Drummond. 2006. Multiscale *Cryptosporidium*/sand interactions in water treatment. Water Res. 40:3315–3331.

Tufenkji, N., and M. Elimelech. 2004. Correlation equation for predicting single-collector efficiency in physiochemical filtration in saturated porous media. Environ. Sci. Technol. 38:529–536.

Tufenkji, N., and M. Elimelech. 2005a. Breakdown of colloid filtration theory: Role of the secondary energy minimum and surface charge heterogeneities. Langmuir 21:841–852.

Tufenkji, N., and M. Elimelech. 2005b. Spatial distributions of *Cryptosporidium* oocysts in porous media: Evidence for dual mode deposition. Environ. Sci. Technol. 39:3620–3629.

Tufenkji, N., G.F. Miller, J.N. Ryan, R.W. Harvey, and M. Elimelech. 2004. Transport of *Cryptosporidium* oocysts in porous media: Role of straining and physicochemical filtration. Environ. Sci. Technol. 38:5932–5938.

Tufenkji, N., J.A. Redman, and M. Elimelech. 2003. Interpreting deposition patterns of microbial particles in laboratory-scale column experiments. Environ. Sci. Technol. 37:616–623.

Tufenkji, N., J.N. Ryan, and M. Elimelech. 2002. The promise of bank filtration. Environ. Sci. Technol. 36:A422–A428.

Tuller, M., D. Or, and L.M. Dudley. 1999. Adsorption and capillary condensation in porous media: Liquid retention and interfacial configurations in angular pores. Water Resour. Res. 35:1949–1964.

van Genuchten, M.Th., F.J. Leij, and S.R. Yates. 1991. The RETC code for quantifying the hydraulic functions of unsaturated soils. EPA 600/2-91/065. USEPA, Ada, OK.

van Oss, C.J. 1994. Interfacial forces in aqueous media. Marcel Dekker, New York.

van Oss, C.J. 2006. Interfacial forces in aqueous media. 2nd ed. Taylor & Francis, Boca Raton, FL.

van Oss, C.J., M.K. Chaudhury, and R.J. Good. 1988. Interfacial Lifshitz–van der Waals and polar interactions in macroscopic systems. Chem. Rev. 88:927–941.

Veerapaneni, S., J. Wan, and T.K. Tokunaga. 2000. Motion of particles in film flow. Environ. Sci. Technol. 34:2465–2471.

Verwey, E.J.W., and J.Th.G. Overbeek. 1948. Theory of the stability of lyophobic colloids. Elsevier, Amsterdam.

Vidali, M. 2001. Bioremediation: An overview. Pure Appl. Chem. 73:1163–1172.

Wan, J., and T.K. Tokunaga. 1997. Film straining of colloids in unsaturated porous media: Conceptual model and experimental testing. Environ. Sci. Technol. 31:2413–2420.

Wan, J.M., and T.K. Tokunaga. 2002. Partitioning of clay colloids at air–water interfaces. J. Colloid Interface Sci. 247:54–61.

Wan, J., and T.K. Tokunaga. 2005. Comments on "Pore-scale visualization of colloid transport and retention in partly saturated porous media." Vadose Zone J. 4:954–956.

Wan, J., and J.L. Wilson. 1994a. Visualization of the role of the gas–water interface on the fate and transport of colloids in porous media. Water Resour. Res. 30:11–23.

Wan, J., and J.L. Wilson. 1994b. Colloid transport in unsaturated porous media. Water Resour. Res. 30:857–864.

Weiss, W.J., E.J. Bouwer, R. Aboytes, M.W. LeChevallier, C.R. O'Melia, B.T. Le, and K.J. Schwab. 2005. Riverbank filtration for control of microorganisms: Results from field monitoring. Water Res. 39:1990–2001.

Xu, S., B. Gao, and J.E. Saiers. 2006. Straining of colloidal particles in saturated porous media. Water Resour. Res. 42:W12S16, doi:10.1029/2006WR004948.

Yaminsky, V.V., and B.W. Ninham. 1993. Hydrophobic force: Lateral enhancement of subcritical fluctuations. Langmuir 9:3618–3624.

Yao, K.M., M.T. Habibian, and C.R. O'Melia. 1971. Water and waste water filtration: Concepts and applications. Environ. Sci. Technol. 5:1105–1112.

Yoon, J.S., J.T. Germaine, and P.J. Culligan. 2006. Visualization of particle behavior with a porous medium: Mechanisms for particle filtration and retardation during downward transport. Water Resour. Res. 42:W06417, doi:10.1029/2004WR003660.

Yoon, R.-H., D.H. Flinn, and Y.I. Rabinovich. 1997. Hydrophobic interactions between dissimilar surfaces. J. Colloid Interface Sci. 185:363–370.

Yoon, R.-H., and S.A. Ravishankar. 1996. Long-range hydrophobic forces between mica surfaces in alkaline dodecylammonium chloride solutions. J. Colloid Interface Sci. 179:403–411.

Zevi, Y., A. Dathe, J.F. McCarthy, B.K. Richards, and T.S. Steenhuis. 2005. Distribution of colloid particles onto interfaces in partially saturated sand. Environ. Sci. Technol. 39:7055–7064.

Zhang, L., L. Ren, and S. Hartland. 1996. More convenient and suitable methods for sphere tensiometry. J. Colloid Interface Sci. 180:493–503.

Zhang, P., W.P. Johnson, T.D. Scheibe, K. Choi, F.C. Dobbs, and B.J. Mailloux. 2001. Extended tailing of bacteria following breakthrough at the Narrow Channel Focus Area, Oyster, Virginia. Water Resour. Res. 37:2687–2698.

Zhuang, J., J.F. McCarthy, J.S. Tyner, E. Perfect, and M. Flury. 2007. In-situ colloid mobilization in Hanford sediments under unsaturated transient flow conditions: Effect of irrigation pattern. Environ. Sci. Technol. 41:3199–3204.